MR Imaging of Hepatocellular Carcinoma in the Cirrhotic Liver: Challenges and Controversies[1]

Jonathon M. Willatt, MD
Hero K. Hussain, MD
Saroja Adusumilli, MD
Jorge A. Marrero, MD, MS

The incidence of hepatocellular carcinoma (HCC) is expected to increase in the next 2 decades, largely due to hepatitis C infection and secondary cirrhosis. HCC is being detected at an earlier stage owing to the implementation of screening programs. Biopsy is no longer required prior to treatment, and diagnosis of HCC is heavily dependent on imaging characteristics. The most recent recommendations by the American Association for the Study of Liver Diseases (AASLD) state that a diagnosis of HCC can be made if a mass larger than 2 cm shows typical features of HCC (hypervascularity in the arterial phase and washout in the venous phase) at contrast material–enhanced computed tomography or magnetic resonance (MR) imaging or if a mass measuring 1–2 cm shows these features at both modalities. There is an ever-increasing demand on radiologists to detect smaller tumors, when curative therapies are most effective. However, the major difficulty in imaging cirrhosis is the characterization of hypervascular nodules smaller than 2 cm, which often have nonspecific imaging characteristics. The authors present a review of the MR imaging and pathologic features of regenerative nodules and dysplastic nodules and focus on HCC in the cirrhotic liver, with particular reference to small tumors and lesions that may mimic HCC. The authors also review the sensitivity of MR imaging for the detection of these tumors and discuss the staging of HCC and the treatment options in the context of the guidelines of the AASLD and the imaging criteria required by the United Network for Organ Sharing for transplantation. MR findings following ablation and chemoembolization are also reviewed.

[1] From the Departments of Radiology/MRI (J.M.W., H.K.H., S.A.) and Internal Medicine/Hepatology (J.A.M.), University of Michigan Health System, UH-B2A209K, 1500 E Medical Center Dr, Ann Arbor, MI 48109-0030. Received August 2, 2006; revision requested October 3; revision received January 10, 2007; accepted February 22; final version accepted June 8; final review and update by H.K.H. November 16. **Address correspondence to** H.K.H. (e-mail: *hhussain@umich.edu*).

Hepatocellular carcinoma (HCC) is the fifth most common tumor in the world and is the third most common cause of cancer-related death, after lung and stomach cancer (1). Until recently, the incidence and mortality rates for HCC in the United States were consistently low. Since the mid-1990s, however, the incidence of HCC has risen rapidly, and it is expected to increase in the next 2 decades (2,3). The average annual age-adjusted incidence of HCC increased from 1.3 per 100 000 in 1981–1983 to 3.0 per 100 000 in 1996–1998, with a 25% increase observed between 1993 and 1998 (4). According to a recent annual report to the nation on cancer (5), HCC is second only to thyroid cancer in increase in incidence rates from 1994 to 2003. This is largely attributed to hepatitis C virus infection (3,6–10).

Essentials

- The 5-year survival rate of patients undergoing curative therapies for hepatocellular carcinoma (HCC) ranges 40%–75%.
- Most HCCs develop by means of a multistep progression: from a low-grade dysplastic nodule to a high-grade dysplastic nodule, to a dysplastic nodule with a focus of HCC, and finally to overt carcinoma.
- Criteria favoring malignancy are size larger than 2 cm, delayed hypointensity "washout," hyperintensity at T2-weighted imaging, delayed enhancing tumor capsule, and rapid interval growth.
- Patients are selected for transplantation, resection, ablation, chemoembolization, or palliative treatments on the basis of the Barcelona Clinic Liver Cancer staging system, which was recently endorsed by both European and American liver disease organizations.
- Priority allocation of donor livers is based on the Model for End-stage Liver Disease score, which is a predictor of mortality within 3 months.

Cirrhosis is the strongest predisposing factor for HCC, with approximately 80% of cases of HCC developing in a cirrhotic liver (6). The annual incidence of HCC is 2.0%–6.6% in patients with cirrhosis compared with 0.4% in patients without cirrhosis (6). The most common etiologic agent is hepatitis B virus infection in Asia and Africa (11,12). Up to 30% of patients with chronic hepatitis B virus infection can develop HCC without cirrhosis (13–15). In the West and in Japan, hepatitis C virus infection is the main risk factor for cirrhosis and is associated with the highest HCC incidence (5-year cumulative incidence: 30% in Japan and 17% in the West). Other less common causes of cirrhosis have variable, but usually lower, rates of HCC. The 5-year cumulative HCC risk is 21% in hereditary hemochromatosis, 10% in hepatitis B virus infection (up to 15% in high endemic areas), 8% in alcoholic cirrhosis, and 5% in biliary cirrhosis (10). In viral-related cirrhosis, coinfection with other viruses and alcohol abuse significantly increase the risk of HCC (10). Cryptogenic cirrhosis accounts for 5%–30% of cases of end stage liver disease (2), and it has been suggested that many of these cases represent the more severe form of nonalcoholic fatty liver disease, nonalcoholic steatohepatitis, which can lead to liver fibrosis, cirrhosis, and subsequently to HCC (2,16).

HCC meets the criteria established by the World Health Organization for performing surveillance (17). The 5-year survival rates of patients undergoing curative therapies for HCC, including liver transplantation, hepatic resection, and percutaneous ablative techniques, range between 40% and 75% (18). Therefore, by screening populations at risk for HCC (ie, patients with cirrhosis), early stage tumors can be detected and curative therapy can be initiated. It is estimated that about 30% of patients with HCC are candidates for such curative interventions. The current screening tests clinically available for patients with cirrhosis are α-fetoprotein (AFP) level testing and ultrasonography (US) (19). The performance characteristics of these tests in cohort or case-control studies have yielded sensitivities of 50%–60% (20). A recent randomized controlled trial showed that AFP and US screening reduce mortality (21).

In the event of abnormal results at surveillance US or AFP level testing (>20 ng/mL [20 μg/L]), contrast material–enhanced magnetic resonance (MR) imaging or computed tomography (CT) are the best imaging techniques currently available for the noninvasive diagnosis of HCC. The detection of small tumors, however, remains the most challenging area in imaging the cirrhotic liver. MR imaging outperforms CT in this area, although the sensitivities of both tests remain disappointing; the pooled estimate of the sensitivity for detection of HCC is 81% for MR imaging compared with 68% for CT (22). Diagnostic confirmation and assessment of disease extent were previously dependent on percutaneous biopsy findings and on invasive procedures such as angiography and lipiodol CT (23). More recent advances in imaging technology, as well as changes in diagnostic criteria, have brought imaging to the forefront as well as under greater scrutiny.

In this review, we focus on MR imaging features of HCC in the cirrhotic liver, diagnostic dilemmas, staging and treatment options, and imaging after treatment. We also address the issue of small hypervascular nodules that are difficult to characterize at imaging and that constitute the major challenge in imaging of the cirrhotic liver.

Published online
10.1148/radiol.2472061331

Radiology 2008; 247:311–330

Abbreviations:
AASLD = American Association for the Study of Liver Diseases
AFP = α-fetoprotein
BCLC = Barcelona Clinic Liver Cancer
FSE = fast spin echo
HCC = hepatocellular carcinoma
RFA = radiofrequency ablation
SPGR = spoiled gradient-recalled acquisition in the steady state
UNOS = United Network for Organ Sharing

Authors stated no financial relationship to disclose.

MR Imaging Features of Cirrhotic Nodules

Cirrhosis is the end result of chronic liver disease. It is characterized by destruction of the normal hepatic architecture, which is replaced by fibrous septa and a spectrum of nodules ranging from benign regenerative nodules to HCC (24,25).

The development of HCC in the cirrhotic liver is described either as de novo hepatocarcinogenesis or as a multistep progression, from low-grade dysplastic nodule to high-grade dysplastic nodule, then to dysplastic nodule with microscopic foci of HCC, then to small HCC, and finally to overt carcinoma (26,27). Patients with high-grade dysplastic nodules are at the greatest risk for HCC (28). It is because of the multistep process that the imaging features of these nodules overlap, particularly with regard to differentiation of dysplastic nodules and small HCCs. The imaging features during the progression to cancer can be largely explained by the changes in the nature of the blood supply to the nodules (27).

Regenerative Nodules

A regenerative nodule is defined as a hepatocellular nodule containing one or more portal tracts located in a liver that is otherwise abnormal due to either cirrhosis or other severe disease (29). These nodules are present in all cirrhotic livers and are surrounded by fibrous septa (29,30). They are also referred to as cirrhotic nodules (29). Cirrhosis is classified, on the basis of the size of these nodules in the pathologic specimen, into micronodular (≤3 mm), macronodular (>3 mm), and mixed types (29). The blood supply of a regenerative nodule continues to be largely from the portal vein, with minimal contribution from the hepatic artery (31). This vascular supply dynamic explains why there is no enhancement during the hepatic arterial phase on MR images, although arterial phase enhancement in regenerative nodules has been described and can be mistaken for HCC (30,32). Large regenerative nodules can measure 5 cm or larger and mimic a mass (29). Because they consist of proliferating normal liver cells surrounded by a fibrous stroma, these nodules are indistinct on T1-weighted and T2-weighted images (25). Less commonly, they can be hyperintense to surrounding liver on T1-weighted images. The exact cause for this hyperintensity is unknown; it may be due to the presence of lipid, protein, or possibly copper (33,34). Regenerative nodules that contain iron (siderotic nodules) may have decreased signal intensity on both T1- and T2-weighted images owing to susceptibility effects (25,35–37) (Fig 1).

Dysplastic Nodules

A dysplastic nodule is defined as a nodule of hepatocytes of at least 1 mm in diameter, with dysplasia of low or high grade but no histologic criteria for malignancy, usually found in a cirrhotic liver (29,38). Dysplastic nodules are found in 15%–25% of cirrhotic livers (39).

Low-grade dysplastic nodules are composed of liver cells with minimal atypia, including slightly increased nuclear/cytoplasmic ratio, minimal nuclear atypia, and absent mitosis (29,38). These nodules are not premalignant. High-grade dysplastic nodules display at least moderate atypia and occasional mitosis (29). They may even express AFP but are not frankly malignant (40). They are considered premalignant, and development of HCC within a dysplastic nodule has been documented within as little as 4 months (41,42). Occasionally, dysplastic nodules can be larger than 2 cm (25). The differentiation of dysplastic nodules from regenerative ones in pathologic specimens can be difficult. However, the cells of regenerative nodules do not display the mildly abnormal features of dysplastic nodules (29,43).

Dysplastic nodules are usually similar in signal intensity to regenerative ones in that they are isointense to surrounding liver on T1- and T2-weighted images. Some dysplastic nodules retain copper, which causes them to have high signal intensity on T1-weighted images (25). If siderotic, these nodules are hypointense to surrounding liver on T1- and T2-weighted images. Low-grade

Figure 1

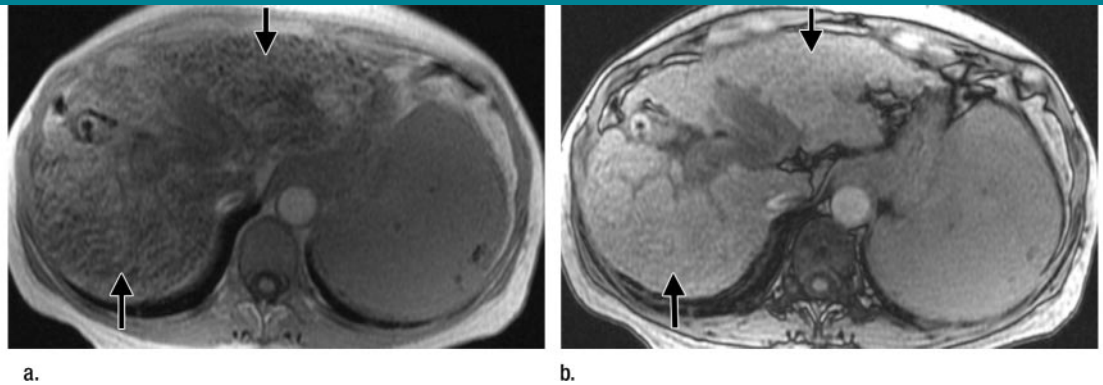

Figure 1: Transverse T1-weighted MR images in 50-year-old woman with cirrhosis secondary to autoimmune hepatitis. There is marked signal intensity loss throughout the hepatic parenchyma (arrows) on the **(a)** in-phase image (repetition time msec/echo time msec, 170/4.4; 70° flip angle) in comparison with the **(b)** opposed-phase image (170/2.2, 70° flip angle), secondary to the presence of siderotic regenerative or dysplastic nodules.

dysplastic nodules are normally supplied by the portal vein and therefore are isointense to liver during the arterial phase. The signal intensity characteristics of some high-grade dysplastic nodules, which receive increasing supply from the hepatic artery (44–47), may overlap with those of HCC nodules during the process of hepatocarcinogenesis. These nodules can enhance in the arterial phase and can be mistaken for HCC. Occasionally, both regenerative and dysplastic nodules can infarct, leading to high signal intensity on T2-weighted images (48). Such nodules are often mistaken for HCC. It has been suggested that both high- and low-grade dysplastic nodules may disappear at follow-up and that only a small percentage of high-grade dysplastic nodules progress to HCC (49).

A dysplastic nodule with a central focus of HCC was first described on T2-weighted images as "a nodule within a nodule" (50). The classic MR appearance is a focus of high signal intensity within a low-signal-intensity nodule on T2-weighted images. This focus of HCC may also enhance in the arterial phase (51).

Regenerative siderotic nodules cannot be distinguished from dysplastic siderotic nodules on MR images (35). Despite earlier suggestions (37), siderotic nodules have not been shown to be associated with an increased incidence of HCC, and the iron content within regenerative and dysplastic nodules is likely a marker for hepatic disease activity rather than a direct cause of carcinogenesis (35,36).

Hepatocellular Carcinoma

HCC is defined as a malignant neoplasm composed of cells with hepatocellular differentiation (29,52). On pathologic specimens, HCC is macroscopically classified as "massive" when there is a single large mass with or without small satellite nodules; as "nodular" when there are multiple, fairly discrete nodules throughout the liver; or as "diffuse" when there are multiple, minute indistinct nodules throughout the liver (52). Small HCC is defined as a tumor measuring 2 cm or smaller (29,52).

HCC has variable signal intensity on T1- and T2-weighted images (53,54). High signal intensity on T1-weighted images is attributed to intratumoral fat, to copper or glycogen, or to zinc in the surrounding parenchyma (53,55). Fat content leads to signal intensity loss at opposed-phase imaging (56). Moderate high signal intensity on T2-weighted images is quite specific for HCC, since dysplastic nodules are not hyperintense unless they are infarcted (25,48,53). However, HCC can be difficult to detect on T2-weighted images because of heterogeneity of the cirrhotic liver, which obscures mildly hyperintense and isointense tumors. Breathing artifacts, particularly in patients with ascites, can also create difficulty in detection (57,58).

With regard to the stepwise development of HCC, studies based on findings at CT during arterial portography and CT during hepatic arteriography with pathologic correlation have shown that as the grade of malignancy within the nodules evolves, there is gradual reduction of the normal hepatic arterial and portal venous supply to the nodule followed by an increase in the abnormal arterial supply via newly formed abnormal arteries (neoangiogenesis) (59). Histopathologically, this corresponds to a diminution in the portal tracts (portal vein and hepatic artery), which are virtually absent in HCC (59). Moreover, unpaired arteries and sinusoidal capillarization are most common in HCC, less common in dysplastic nodules, and rare in regenerative nodules (60).

This process of neoangiogenesis or arterial recruitment dictates the main imaging feature of HCC, which is arterial enhancement (61,62). Arterial enhancement (hypervascularity) (54,63) is considered an essential characteristic of HCC and is used as the only radiologic feature on contrast-enhanced CT or MR images for the noninvasive diagnosis of HCC by the United Network for Organ Sharing (UNOS) prior to listing (64). Arterial enhancement of HCC relative to surrounding parenchyma is often moderate in comparison with the enhancement of other hypervascular lesions, such as hemangioma and focal nodular hyperplasia. Enhancement is heterogeneous in large lesions and is homogeneous in small lesions (54,65). In a large multi-institutional study of the imaging features of HCC, Kelekis et al (54) found that the most common appearance of HCC on MR images is hypointensity at T1-weighted imaging, hyperintensity at T2-weighted imaging, and diffuse heterogeneous arterial enhancement with venous washout (Fig 2). However, they also found that small HCCs measuring 1.5 cm or smaller are frequently isointense on T1- and T2-weighted images and are detected only in the arterial phase (Fig 2). Unfortunately, some HCCs also display hyperintense signal intensity on T1-weighted images and hypointense signal intensity on T2-weighted images, mimicking dysplastic nodules (25,54). Enhancement in the arterial phase remains a distinguishing feature.

There is some debate as to whether more than one arterial phase is needed to detect the transient arterial blush of HCC, which can be brief. Given the variability in cardiovascular dynamics, there is concern that tumors can be missed, and up to six sequences have been proposed to minimize this (66–69).

Tumors usually become hypointense in the portal venous and delayed phases and often show a delayed enhancing outer rim "capsule" (hereafter, delayed enhancing capsule). These features are highly specific for HCC (25,32), with a reported overall sensitivity of 89% and specificity of 96% for delayed hypointensity (62). Rarely, HCC may remain hyperintense relative to adjacent liver parenchyma on venous and delayed phase images.

Occasionally, early stage HCC, especially tumors smaller than 2 cm, can be isointense or hypointense in the arterial phase. This probably reflects the stage of carcinogenesis within the nodule where there has been partial or complete loss of the normal portal tract, with no associated increased arterialization to cause hyperintensity in the arterial phase (59,70).

Histologically and radiologically, it can be difficult to differentiate some

Radiology

Figure 2

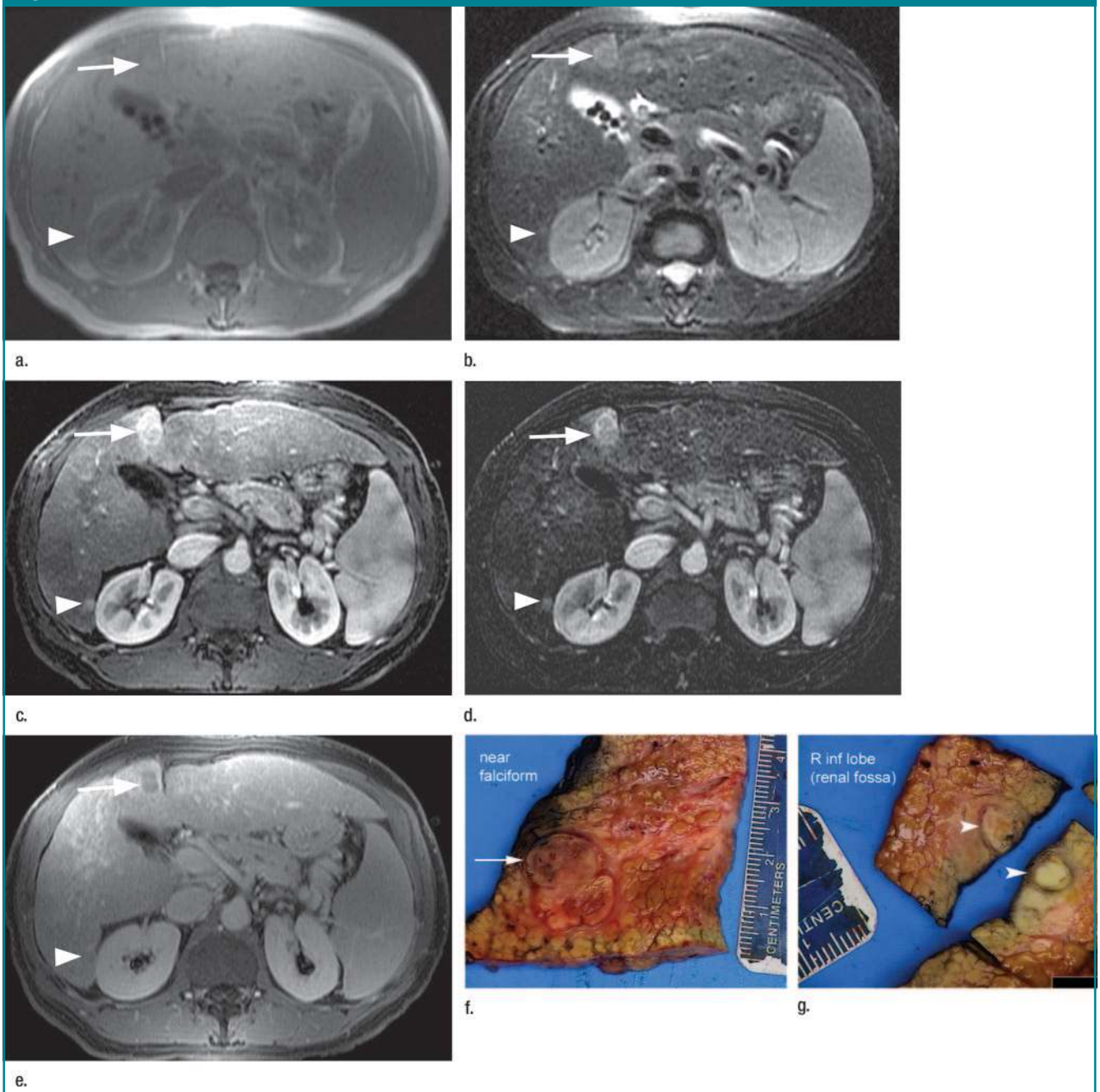

Figure 2: Transverse MR and pathologic images in 61-year-old man with hepatitis C–related cirrhosis. A 3-cm lesion (arrow) near the falciform ligament is minimally hyperintense to adjacent parenchyma on **(a)** T1-weighted in-phase image (160/4.4) and hyperintense on **(b)** T2-weighted fast-recovery fast spin-echo (FSE) image (2870/87). The lesion is hypervascular on **(c)** arterial-phase T1-weighted three-dimensional spoiled gradient echo image (spoiled gradient-recalled acquisition in the steady state [SPGR]) with fat saturation (3.6/1.3, 12° flip angle) and **(d)** subtracted image (arterial phase image minus precontrast image) and becomes hypointense on **(e)** delayed phase image. **(f)** Explant specimen confirms HCC near the falciform ligament, which has typical imaging appearance. A second lesion (arrowhead, **a**–**e**) measuring 1 cm, in the inferior right lobe of the liver, adjacent to the renal fossa, is isointense on **a** and mildly hyperintense on **b**. The lesion enhances on **c** and is seen on **d**. It becomes isointense to parenchyma in **e**. Hyperintensity at T2-weighted imaging increases the specificity of diagnosis of HCC in this small hypervascular lesion. **(g)** Pathologic specimen confirms HCC (arrowheads) in the inferior right lobe adjacent to renal fossa. The tumor has been bisected. Note incidental gallstones.

dysplastic nodules and small HCCs. Radiologic criteria favoring malignancy are as follows: size larger than 2 cm, hyperintensity at T2-weighted imaging, delayed hypointensity "washout," delayed enhancing tumor capsule, and rapid interval growth (25). Subtraction techniques can be useful to assess enhancement in nodules that are of high signal intensity on T1-weighted images before contrast material enhancement.

Certain morphologic features help distinguish HCC from nontumorous arterially enhancing nodules. These nodules are also referred to in the literature as nonspecific arterially enhancing lesions or nodules, nonneoplastic hepatic arterial phase enhancing lesions, arterial enhancing pseudolesions, and transient hepatic attenuation (intensity) difference (62,71–73). These terms refer to a variety of nonspecific entities that demonstrate some similarities to HCC in terms of arterial hypervascularity (74). Delayed hypointensity of an arterially enhancing lesion is an important feature that increases the specificity of the diagnosis of HCC, especially for lesions smaller than 2 cm for which the reported sensitivity and specificity are 80% and 95%, respectively (62,75–78). However, the absence of delayed hypointensity does not exclude malignancy, since some early tumors as well as dysplastic nodules have residual portal venous supply and remain isointense to liver parenchyma (Fig 2).

Ueda et al (79), in a study of 32 HCCs (mean diameter, 2.5 cm) at single-level dynamic CT hepatic arteriography, found that all tumors had a surrounding halo of enhancement or "corona enhancement" in the venous phase. This useful sign is related to the portal venous drainage of the tumor, but this technique has limited value in daily practice because it is invasive, expensive, and limited to the assessment of a single lesion, and it cannot be used to evaluate the entire liver. The portal venous drainage of HCC may explain the high incidence of portal vein thrombosis associated with this tumor.

Large HCCs are characterized by a more variable pattern. A mosaic pattern is created by confluent nodules separated by fibrous septa and areas of necrosis. These tumors are usually of high signal intensity on T2-weighted images and enhance heterogeneously (69,80). Large HCCs (>2 cm) do not pose a diagnostic problem. The main difficulty in imaging the cirrhotic liver is determining the cause of small (<2 cm) arterially enhancing nodules.

Diffuse-type HCC constitutes up to 13% of cases of HCC (81) and appears as an extensive, heterogeneous, permeative hepatic tumor with portal venous

Figure 3

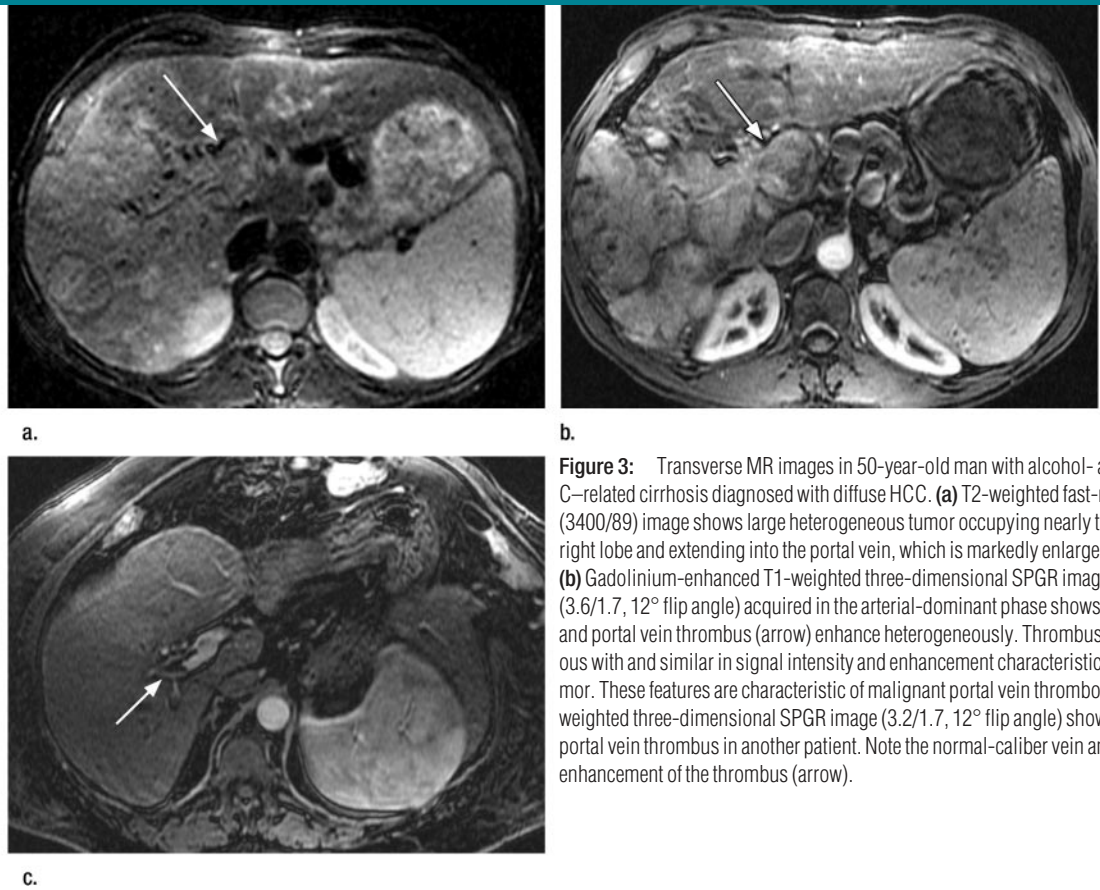

Figure 3: Transverse MR images in 50-year-old man with alcohol- and hepatitis C–related cirrhosis diagnosed with diffuse HCC. **(a)** T2-weighted fast-recovery FSE (3400/89) image shows large heterogeneous tumor occupying nearly the entire right lobe and extending into the portal vein, which is markedly enlarged (arrow). **(b)** Gadolinium-enhanced T1-weighted three-dimensional SPGR image (3.6/1.7, 12° flip angle) acquired in the arterial-dominant phase shows that tumor and portal vein thrombus (arrow) enhance heterogeneously. Thrombus is contiguous with and similar in signal intensity and enhancement characteristics to the tumor. These features are characteristic of malignant portal vein thrombosis. **(c)** T1-weighted three-dimensional SPGR image (3.2/1.7, 12° flip angle) shows bland portal vein thrombus in another patient. Note the normal-caliber vein and lack of enhancement of the thrombus (arrow).

tumor thrombosis (Fig 3), often associated with an elevated serum AFP level. These tumors have a patchy or nodular early enhancement pattern and can be difficult to detect on T1- or T2-weighted images, but they become hypointense in the late phases of enhancement (81).

Portal vein invasion is another important feature of HCC and is thought to be related to the portal venous drainage of HCC (79). However, patients with cirrhosis can also develop benign portal vein thrombosis secondary to portal hypertension and venous stasis (82). The prevalence of nonmalignant portal vein thrombosis in cirrhosis ranges from 0.65% to 15.8% (83,84). Malignant portal vein thrombosis in HCC occurs by means of direct invasion of the vein (82). The reported incidence of malignant portal vein thrombosis in association with HCC ranges from 5% to 44% (85–88). Higher rates have been reported at autopsy (89). A malignant thrombus is always contiguous with or directly in contact with a parenchymal tumor (Fig 3a, 3b). Increased T2-weighted signal intensity is highly suggestive of malignant thrombosis. Malignant portal vein thrombosis is characterized by dramatic expansion of the vein, compared with near-normal–caliber veins in bland thrombosis (90) (Fig 3c). The presence of neovascularity is also highly specific for malignant thrombosis (90), and assessment of the dynamic gadolinium-enhanced gradient-echo images can help distinguish between the two. A bland thrombus has very low signal intensity due to hemosiderin content, whereas malignant thrombus has the same signal intensity and contrast enhancement pattern as the tumor (91). Rarely, benign thrombi may also show contrast enhancement (90). While macrovascular invasion can be easily detected at imaging, microvascular invasion is almost impossible to visualize, but, fortunately, it does not constitute a contraindication to curative treatments (64). Nevertheless, microvascular invasion is often associated with tumor recurrence following resection or transplantation (92–95). Extension of HCC into the hepatic veins occurs less frequently than and is often associated with invasion of the portal vein. Rarely, HCC may grow in major bile ducts, causing obstructive jaundice, and is frequently associated with concomitant intraportal tumor growth (89).

The term *transient hepatic intensity difference* (THID), a modification of the CT term *transient hepatic attenuation difference*, is also used to describe peritumoral enhancement, which is seen around HCC as an area of hypervascularity in the arterial phase (96). It can result from compensatory increased arterial supply to a region owing to reduced portal supply from either malignant occlusion or compression of the portal vein. In these cases, the THID is usually wedge shaped and conforms to the segment or lobe with reduced portal supply (97). Peritumoral enhancement can be secondary to arterioportal shunting, which can occur spontaneously within HCC or following interventional procedures such as biopsy or ablation (74,96). Peritumoral enhancement in these cases can be ill defined and result in overestimation of the size of tumor in the arterial phase, which may influence transplantation decisions. Comparing the arterial phase with the delayed phases and the T1- and T2-weighted images is necessary to determine the most accurate tumor measurement.

Lesions Mimicking HCC

While considered the most consistent feature of HCC, arterial enhancement is a feature of other nonmalignant lesions that can be found in the cirrhotic liver, especially those measuring smaller than 2 cm, which explains the high incidence of false-positive results for HCC (98–100). Transient arterial enhancement due to nontumorous arterioportal shunts (101,102) or focal obstruction of a distal parenchymal portal vein (103) is often seen in the cirrhotic liver. Usually these shunts are isointense to surrounding parenchyma on T1- and T2-weighted images, but occasionally they can be minimally hyperintense on T2-weighted images and associated with mild prolonged parenchymal enhancement (101,102). Shunts are commonly peripheral and wedge shaped but can be nodular or irregularly outlined and do not displace internal vasculature (101,103). Small arteriovenous shunts and pseudoaneurysms can occur following biopsy and exhibit enhancement that matches blood pooling on contrast-enhanced images (30). Aberrant venous drainage and early drainage by a subcapsular vein have all been described as hypervascular areas mimicking small HCCs (74,101).

Fibrosis is present with cirrhosis usually in a lattice-like network throughout the liver. Focal confluent hepatic fibrosis, which is observed in end-stage liver disease, can be masslike and mistaken for HCC, especially in cirrhosis secondary to primary sclerosing cholangitis (104). Areas of confluent fibrosis can be diffuse but more often they are focal, wedge shaped with the wide base toward the liver capsule, and usually located in the anterior and medial segments of the liver, either involving the entire segment or a portion of it (104). Confluent fibrosis is usually associated with atrophy of the affected segment, and capsular retraction over the area is common (30). Confluent fibrosis is usually of low signal intensity relative to the liver on T1-weighted images and hyperintense on T2-weighted images. Delayed contrast enhancement of fibrosis is characteristic, but occasionally confluent fibrosis shows contrast enhancement in the arterial phase, simulating a neoplasm and requiring biopsy for confirmation (104,105) (Fig 4). The characteristic shape, location, volume loss, and enhancement can help differentiate focal fibrosis from a tumor (106).

Hemangiomas, commonly found in normal livers, are rare in end-stage cirrhosis, probably because the process of cirrhosis obliterates existing hemangiomas. Thus, hemangiomas are often atypical in appearance in cirrhotic livers and contain large regions of fibrosis (104) (Fig 5). Small cysts are often seen in cirrhosis and do not pose a diagnostic challenge. Peribiliary cysts are usually arranged along the walls of large bile ducts and occur as a result of obstruction of peribiliary glands in the duct wall or within periductal tissue. Except for their unique location, they appear as simple cysts with low signal intensity on

T1-weighted images, high signal intensity on T2-weighted images, and no enhancement (107).

Other lesions such as focal nodular hyperplasia (FNH) or FNH-like nodules, hepatic adenoma, and hypervascular metastases are rare in the cirrhotic liver but can be difficult to distinguish from HCC (108–110). It is important to distinguish HCC from benign large regenerative nodules, which occur secondary to liver damage without cirrhosis, for example in the setting of Budd-Chiari syndrome, or severe disease of the portal veins or hepatic sinusoids. These nodules often appear as multiple well-defined arterially enhancing nodules with high signal intensity on T2-weighted images and sometimes delayed hypointensity (111–112). They sometimes contain a central scar (113). Knowledge of the patient's history is helpful. Unlike regenerative nodules of cirrhosis, regenerative nodules in Budd-Chiari syndrome do not have fibrosis around the nodules (29).

Intrahepatic cholangiocarcinoma is

Figure 4

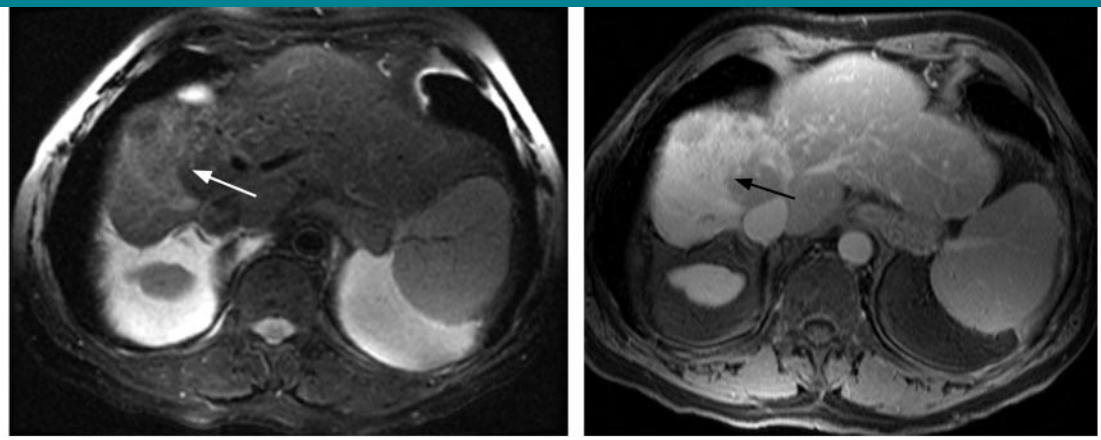

a. b.

Figure 4: Transverse MR images in 72-year-old man with alcohol-related cirrhosis. There is confluent hepatic fibrosis (arrow), which is seen as a wedge-shaped area of increased signal intensity on **(a)** T2-weighted fast-recovery FSE (3200/92) image, associated with capsular retraction. The area of fibrosis shows intense delayed enhancement relative to adjacent parenchyma on **(b)** T1-weighted SPGR image (155/1.3, 70° flip angle) acquired in the venous phase. This morphology and pattern of enhancement is atypical for HCC.

Figure 5

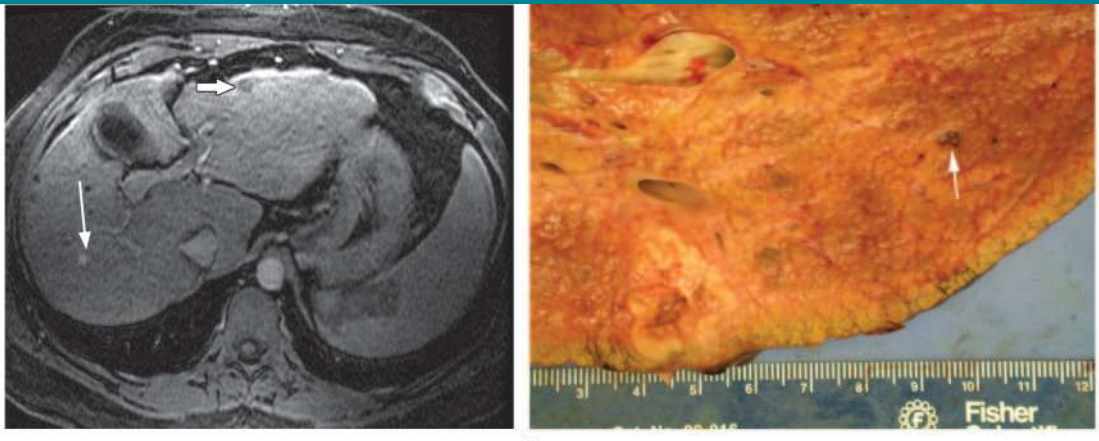

a. b.

Figure 5: Images in 46-year-old man with hepatitis C–related cirrhosis. **(a)** Arterial-dominant phase transverse T1-weighted three-dimensional SPGR MR image (3.6/1.7, 12° flip angle) shows a 6-mm nonspecific hypervascular lesion (thin arrow). This patient has a dominant 5-cm HCC (not shown). A small nodule in the anterior lateral segment of the left lobe (thick arrow) was found to be a cirrhotic nodule. **(b)** At explant evaluation, the tiny hypervascular lesion was found to be a hemangioma (arrow).

also occasionally difficult to distinguish from HCC. Intrahepatic cholangiocarcinoma usually shows thin or thick rim enhancement in the arterial and venous phases, with progressive and concentric filling of contrast material in the later phases. This pattern of enhancement is atypical for HCC. Intrahepatic biliary duct dilation distal to the tumor and associated capsular retraction are features more commonly associated with intrahepatic cholangiocarcinoma and are rarely seen in association with HCC (114,115). Narrowing or obstruction of the portal vein associated with intrahepatic cholangiocarcinoma is usually due to external compression (114).

Imaging Technique

Imaging of the cirrhotic liver can be performed at 1.5-T and 3.0-T field strengths (116). A phased-array coil should routinely be used. The protocol for imaging the cirrhotic liver should always include T1-weighted gradient-recalled echo (GRE) in-phase and opposed-phase sequences, a moderately T2-weighted FSE sequence or a variant such as fast-recovery FSE with an echo time of 80–90 msec (a short inversion time inversion-recovery sequence can be used instead), and multiphase T1-weighted dynamic gadolinium-enhanced sequences. A heavily T2-weighted sequence (echo time, ≥120 msec) helps distinguish between cystic and solid lesions and a fast sequence, such as single-shot FSE (or half-Fourier acquisition turbo spin-echo—half-Fourier rapid acquisition with relaxation enhancement), is used for this purpose.

The sequences used can vary according to vendor and personal preferences (117), but certain guidelines should be followed: First, to improve image quality, sequences should be performed during suspended respiration or should be respiratory averaged (some T2-weighted sequences). Suspending respiration at end expiration produces more consistent breath holding compared with end inspiration but is more difficult for patients (118). Second, GRE sequences have replaced spin-echo sequences for T1-weighted imaging; using a dual-echo sequence that allows simultaneous acquisition of the earliest opposed-phase and in-phase images minimizes misregistration and improves the characterization of focal lesions and diffuse liver disease (119,120). The acquisition of the earliest opposed-phase echo (2.2 msec at 1.5-T and 1.15 msec at 3-T imaging) followed by the subsequent in-phase echo enables the distinction between signal intensity loss caused by the presence of lipid seen on opposed-phase images and signal intensity loss due to susceptibility artifact from hepatic iron deposition, which is exaggerated on the longer of the two echoes (usually in phase). Third, three-dimensional gadolinium-enhanced GRE sequences are preferred to two-dimensional GRE sequences because of the thinner sections obtained, which improve lesion detection and permit multiplanar image reconstructions for presurgical planning (121–124). Section thickness should not exceed 4 mm for three-dimensional sequences and 6 mm for two-dimensional sequences. Fourth, contrast agent bolus timing is strongly recommended, based on our experience and review of the literature, to ensure the consistent capturing of the arterial-dominant phase; fixed delay is not a reliable method in this patient population. Options include use of a test bolus (125) and various automated detection methods (126). Hypervascular HCC is most conspicuous in the middle arterial phase and can be missed if the arterial-dominant phase images are acquired early (127). A timing bolus is not essential if rapid multiphase arterial imaging is performed. Fifth, to improve lesion characterization—for example, to detect washout or delayed contrast material retention of hemangioma and cholangiocarcinoma—multiphase dynamic gadolinium-enhanced imaging should include three contrast-enhanced phases or more. We routinely acquire four sets of images after gadolinium-based contrast material injection in the arterial-dominant (automated timing, usually 20–35 sec), venous (60–90 sec), interstitial (120–150 sec), and delayed (5 minutes) phases of hepatic enhancement. Last, the highest spatial resolution should be used without compromising signal intensity, taking into account patients' breath-holding capacity. Parallel imaging techniques can be applied to improve spatial resolution and/or reduce acquisition time. However, these techniques should be implemented with care, because they can result in image artifacts and reduced lesion conspicuity (128).

Unenhanced images can be subtracted from arterial-phase gadolinium-enhanced images to assess for arterial enhancement in nodules (129). Subtraction can be performed if the unenhanced and gadolinium-enhanced imaging sequences are identical, if the imager is not retuned between acquisitions, and if there are no image rescaling issues. Acquiring the unenhanced and gadolinium-enhanced images in a single series rather than in separate series minimizes these differences and is possible with most imagers. Patients should be instructed to hold their breath in a similar fashion during all sequences to minimize misregistration artifacts, which appear as a bright line at the edge of organs owing to incomplete overlap.

Sensitivity of MR Imaging

Pooled estimates of the sensitivities and specificities of gadolinium-enhanced (gadodiamide and gadopentetate dimeglumine) and iron oxide–enhanced MR imaging for the detection of HCC are 81% and 85%, respectively, compared with 68% and 93% for contrast-enhanced helical CT (22). MR imaging is sensitive for the detection of lesions measuring 2 cm or larger but is insensitive for the diagnosis of small HCC (<2 cm) and carcinomatosis (99,130). Reported sensitivities of two- and three-dimensional gadolinium-enhanced MR imaging for the detection of HCC on a per nodule basis are 33%–90% for HCCs of all sizes (99,130–137), 50%–80% for HCCs of 2 cm or smaller, and 4%–33% for HCC smaller than 1 cm (99,130,131,133,135,136).

Several studies have compared gadolinium-enhanced MR imaging with contrast-enhanced helical CT for the de-

tection of HCC. Some studies have reported higher sensitivities of MR imaging compared with CT for HCC of all sizes (reported sensitivities of 76% vs 61% [131], 61% vs 52% [132], 90% vs 78% [133], and 77% vs 54% [134] for MR imaging and CT, respectively) and for HCC measuring 1–2 cm (reported sensitivities of 84% vs 47% [131] and 85% vs 68% [133], respectively). Other studies have reported either no significant difference between the two modalities or slightly better performance of CT (reported sensitivities of 63% vs 66% [135], 48% vs 47% [136], and 50%–56% vs 56%–67% [138] for MR imaging and CT, respectively). Of note, the three-dimensional gadolinium-enhanced sequence used in a study by Burrel et al (131) was optimized for MR angiography by using a higher flip angle to increase lesion conspicuity.

Contrast agents other than gadolinium-based contrast media have been used for imaging HCC. Superparamagnetic iron oxide particles used alone (139) or in conjunction with gadolinium-based contrast agents (140,141) have been shown to be highly sensitive for the detection of HCC, particularly for small tumors. The reported sensitivity of double-contrast MR imaging for the detection of HCC measuring 1–2 cm is 92% (140,141).

Staging of HCC

Clinical staging of cancers provides a guide to assess prognosis and to direct therapeutic interventions. Several staging systems have been proposed for HCC, such as the modified TNM, Barcelona Clinic Liver Cancer (BCLC), Okuda, and other classification systems (142). UNOS, which is the organization that coordinates U.S. organ transplant activities, uses the modified TNM staging system for HCC to determine eligibility for liver transplantation (64). Patients with modified TNM stage II HCC (a single tumor of 2 to <5 cm and no more than three tumors, all <3.0 cm) with no extrahepatic spread and/or macrovascular involvement (ie, portal or hepatic veins) are eligible for liver transplantation (64). The modified TNM classification corresponds to the Milan criteria for HCC (143), which have been widely used as the guidelines for selection of patients for transplantation in many centers. The Milan criteria were embraced after results of a study by Mazzaferro et al (143) showed excellent overall and recurrence-free survival rates of 85% and 92%, respectively, at 4 years after orthotopic liver transplantation in 35 patients with solitary HCC not exceeding 5 cm in maximal diameter or no more than three tumors, with none larger than 3 cm.

However, unlike with most cancers, staging of HCC is not simply a process of measuring tumor extent, nodal involvement, and metastasis or of assessing the aggressiveness of the tumor by means of its histologic characteristics. The staging of HCC, particularly in the context of assessment for resection or for transplantation, is complicated by the fact that HCC almost always is found on the background of cirrhosis, and therefore liver function has to be taken into account. For this reason the staging process is complicated, and several different systems have been proposed.

The better staging system for HCC has been shown to include tumor burden, hepatic function, and overall patient health and has a link to treatment (23,142,144). The only staging system that includes these criteria is the BCLC system, which is also the only system validated in other populations (142,145,146). The BCLC system was recently endorsed by the 2005 European Association for the Study of the Liver and by the American Association for the Study of Liver Diseases (AASLD) and appears in the AASLD practice guidelines (20).

The BCLC staging system is linked to an evidence-based treatment strategy (147): Radical approaches, including resection and transplantation, are offered to patients at stage 0 (HCC < 2 cm without vascular invasion or spread) and stage A (solitary tumor ≤5 cm or up to three nodules, each ≤3 cm). If radical therapies are not feasible, patients are evaluated for percutaneous ablative treatments. With this strategy the expected 5-year survival is between 50% and 75%. Chemoembolization is offered to patients with stage B disease (large or multinodular HCC without vascular invasion, extrahepatic spread, or cancer-related symptoms), particularly those with compensated cirrhosis. The expected 3-year survival for these patients may exceed 50%. Patients with stage C disease (advanced tumor with vascular involvement, extrahepatic spread, or physical impairment) are entered into research trials to assess new antitumoral agents. Their survival is less than 10% at 3 years. Finally, patients at stage D (with impaired physical status or excessive tumor burden and severe liver impairment) receive symptomatic treatment to minimize their suffering. Their survival at 1 year is also usually less than 10%.

Transplant Allocation Criteria for Patients with Cirrhosis and HCC

Priority allocation of donor livers in the United States is currently based on the Model for End-stage Liver Disease, or MELD, scoring system, which was introduced by UNOS in February 2002 (148). This scoring system was adopted as a predictor of mortality within 3 months for patients with chronic end-stage liver disease (98,149). Each patient with chronic liver disease is given a MELD score, which is based on three biochemical variables: serum bilirubin level, creatinine level, and the international ratio of prothrombin time. Since HCC increases mortality, patients with modified TNM stage II HCC (tumor size ≥2 cm and <5 cm or no more than three tumors, the largest being <3 cm [ie, meet the Milan criteria]) and BCLC stage A who are eligible for orthotopic liver transplantation receive extra points in the MELD scoring system. Their score is equivalent to a 15% probability of candidate death within 3 months of listing (64). This usually raises their priority status on the transplant list. Histopathologic proof of HCC is not required by UNOS for listing if nodules have typical imaging characteristics of HCC. Therefore, imaging has assumed a major role in the diagnosis of HCC in patients with cirrhosis.

One of the UNOS criteria for the diagnosis of HCC is the presence of a "vascular blush" corresponding to the area of suspicion seen at CT or MR imaging (64). Also, prior radiofrequency ablation (RFA), cryoablation, chemical ablation, or chemoembolization can be used as proof of HCC even when there was no histologic confirmation of malignancy prior to the intervention. According to the current AASLD practice guidelines recommendations (20), biopsy is not required when there is a hypervascular mass larger than 2 cm in diameter that shows washout on venous phase images at either CT or MR imaging or when a 1–2 cm mass displays these features at both imaging modalities. Once the diagnosis of TNM stage II HCC is made, the patient receives additional points to elevate his or her priority on the liver transplant waiting list. But for the patient to keep these additional points, tumor presence must be documented every 3 months with CT or MR imaging until the patient receives a transplant organ or the tumor becomes too extensive for transplantation (64). Patients with TNM stage I HCC (single tumor smaller than 2 cm) are no longer eligible for extra points in the MELD scoring system, after approximately one-third of patients with arterially enhancing nodules smaller than 2 cm, presumed to be HCC at imaging, had no tumor at explant pathologic evaluation (98).

Thus, an imaging diagnosis of HCC has a substantial impact on transplant decisions. Radiologists should be aware of this responsibility and must exercise the utmost scrutiny before making a diagnosis of HCC. Erroneous imaging diagnosis of HCC may deny deserving patients the opportunity of a life-saving liver transplantation and may result in unnecessary liver transplantation for others.

The Dilemma of Small (≤2 cm) Arterially Enhancing Lesions

One of the most important roles of imaging in cirrhosis is the detection of HCC. Difficulties in the diagnosis of HCC are posed not by the large lesions but by arterially enhancing nodules smaller than 2 cm in diameter (30,32, 98–100), which often are difficult to characterize as benign or malignant. Small arterially enhancing nodules are not uncommon in the cirrhotic liver, and the majority of these nodules are benign (30,32,71,99,100,150–153). But the most important issue remains the identification of small tumors because curative treatments can be optimally applied to improve outcome (6,154,155). If left alone, these tumors can grow aggressively and invasion can occur before tumors reach the 2-cm cutoff size for small HCC (62). Also, treatment is extremely beneficial in these patients. In patients with cirrhosis and small (<2 cm) HCC, the 5-year survival rate after transplantation is 80% compared with less than 5% in those with untreated symptomatic HCC (6,143,153). Thus every attempt should be made to characterize these nodules. If that is not possible, imaging follow-up or biopsy is used to verify their nature.

The management of small arterially enhancing nodules 1–2 cm is dependent on their imaging features. If the imaging features are highly suggestive of malignancy (delayed hypointensity, delayed enhancing capsule, T2-weighted hyperintensity, or interval growth), the diagnosis of HCC should be made at either imaging or biopsy, because resection or RFA is more effective than surveillance.

More often than not, the imaging features of these nodules are nonspecific, and biopsy or follow-up imaging becomes necessary to verify their nature. Once detected at CT or MR imaging, follow-up imaging of these nodules should be performed with the same imaging modality, because they may not be detected at US. The optimal follow-up interval is yet to be established and is influenced considerably by the tumor volume doubling time. Reported doubling time for HCC ranges from 18 to 605 days. Smaller HCCs have a tendency for faster growth (23,153,156–162). A follow-up interval of 3.0–4.5 months has been suggested. We routinely reimage hypervascular lesions measuring 1–2 cm at 3-month intervals on the basis of the UNOS criteria, which require documentation of tumors every 3 months. Follow-up is particularly useful to document growth, which has been shown to be highly predictive for HCC (151) (Fig 6). However, up to 25% of these arterially enhancing nodules without venous washout remain stable or regress over time (20,71,131,150, 151,163).

While some believe that imaging follow-up of these small nodules in patients with well-compensated cirrhosis is adequate (164,165), others strongly believe in the role of biopsy (166). Biopsy becomes important if the imaging diagnosis of HCC is doubtful, especially in patients who do not require short-term transplantation for the liver disease but in whom the presence of HCC will expedite transplantation owing to the higher mortality associated with malignancy (165).

As for hypervascular nodules smaller than 1 cm detected on contrast-enhanced images, the AASLD recommendations are less clear. In our practice, we follow these nodules at 3–6-month intervals; if the nodules are smaller than 5 mm, subcapsular, wedge shaped, or ill defined, we usually suggest 6-month follow-up. However, when the nodule is round or oval, intraparenchymal, or in the presence of a dominant mass, we perform imaging follow-up at 3-month intervals. It is important to remember that absence of growth during this period does not rule out malignancy, since HCC can grow very slowly. Nodules are declared benign only if they regress or remain stable for 2 years (20). AFP level is not helpful in this situation because of its poor performance as a diagnostic test (167).

MR Imaging and Surgical Resection

Resection is the treatment of choice for noncirrhotic patients with HCC (ie, BCLC stage 0), but patients with cirrhosis and HCC have to be carefully selected to diminish the risk of postoperative liver decompensation and death due to inadequate functional reserve (20).

After resection, the tumor recur-

rence rate exceeds 70% at 5 years owing to dissemination and de novo growth. The best predictors of recurrence are the presence of microvascular invasion at pathologic evaluation and/or additional tumor sites (20, 168–171). The majority of recurrences are due to dissemination and not metachronous tumor. Such recurrences tend to appear during the first 3 years of follow-up and are multifocal (20,172). Continued imaging follow-up is therefore necessary after resection to detect recurrences and tumor seeding, which is another complication of surgery. There is no established optimal imaging follow-up interval. At our institution, we perform MR imaging at 3-month intervals after surgery for all patients whether their preoperative imaging is by means of MR imaging or CT.

MR Imaging and Percutaneous Ablative Techniques

Destruction of tumor cells is achieved by chemical substances (ethanol, acetic acid, boiling saline) or by modifying the temperature (radiofrequency, microwave, laser, cryotherapy).

Percutaneous ethanol injection until recently was the most common treatment for unresectable HCC smaller than 5 cm in size (173). Percutaneous ethanol injection has been superseded by RFA, which enables more effective local control with fewer treatments, but both are effective therapies (174–177). RFA is performed by using a directed alternating current to create local ionic agitation, frictional heat, and ultimately irreversible cell damage (178). Coagulative necrosis is achieved at temperatures that exceed 50°C (179) but usually temperatures up to 100°C are applied. Studies have shown that complete necrosis can be achieved in tumors 5 cm in diameter or smaller, although more than one treatment session may be needed. High success rates have been reported in small (<3 cm) HCC (180). Success rates are lower in larger tumors (181,182). RFA is an effective therapy for preventing or delaying growth of HCC in patients on transplant lists (20,183,184). It can be used to treat early stage HCC in patients who are not resection or transplantation candidates, but its role in downstaging HCC for transplantation has not been established (20,184,185).

The cirrhotic liver lends itself well to RFA because of the hard capsule or pseudocapsule surrounding the tumor that protects the adjacent liver from the effect of local heat (178). RFA is associated with up to 10% adverse effects (186–188). Subcapsular location has been associated with increased risk of peritoneal seeding (186,189) and with a remote risk of capsular rupture and adjacent organ injury (178). Blood circulation within the tumor or in adjacent blood vessels can dissipate heat and reduce the efficacy of therapy (178,190). Other reported complications include hemorrhage, arterioportal shunts, abscess, portal vein thrombosis, ascites, pleural effusion, and adjacent organ injury (178).

Imaging prior to ablation is important to determine the location of the tumor and its proximity to the gallbladder, major vessels, or bile ducts. Following ablation, imaging is often used to assess response and to detect complications and recurrences.

The efficacy of percutaneous ablation is assessed by means of dynamic contrast-enhanced MR imaging or CT 1 month after therapy. Although not entirely reliable, the absence of contrast enhancement within the tumor reflects necrosis, while the persistence of contrast enhancement indicates treatment failure (23). Imaging with MR and CT has been shown to be specific but not sensitive (sensitivity, 36%–89%) for the detection of small foci of residual or recurrent tumor (180,191).

MR imaging features of the RFA

Figure 6

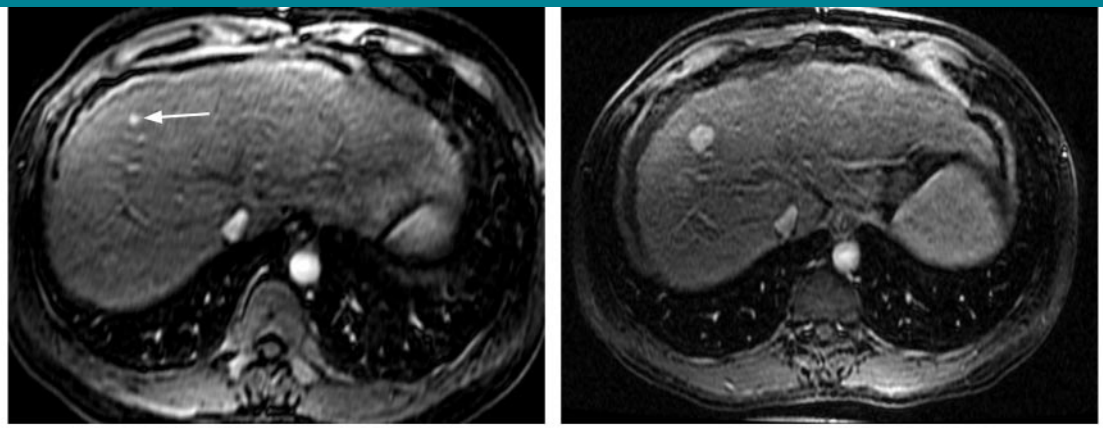

Figure 6: MR images in 44-year-old man with hepatitis C–related cirrhosis and AFP elevated to 20 ng/mL (20 μg/L). **(a)** Arterial-dominant phase transverse T1-weighted three-dimensional SPGR image (3.4/1.7, 12° flip angle) shows 5-mm hypervascular lesion (arrow) without corresponding signal intensity abnormality at other sequences. **(b)** On 6-month follow-up MR image, hypervascular mass enlarged to 1.8 cm; the mass was proved to be an HCC at explant evaluation.

Radiology

Figure 7

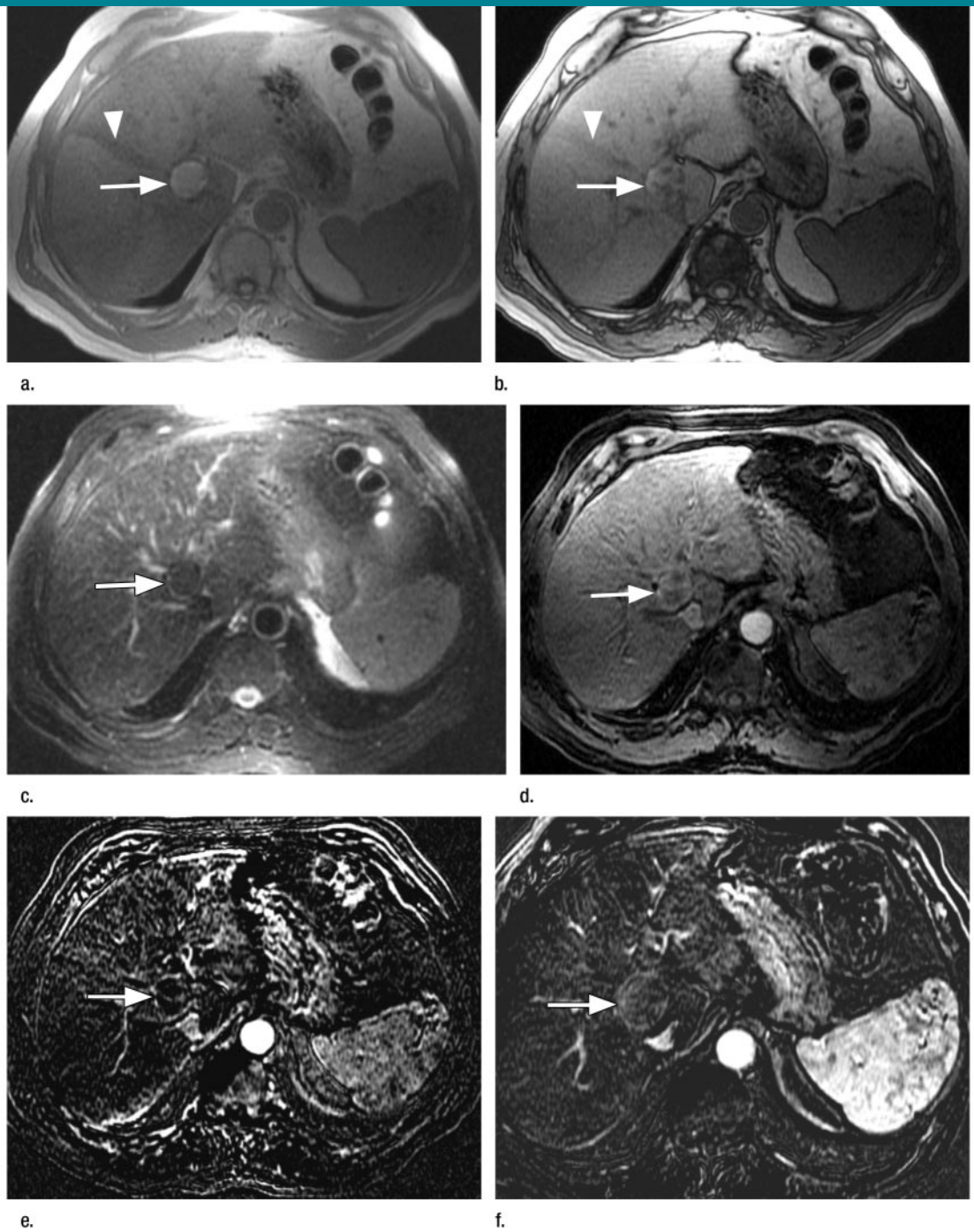

Figure 7: Transverse MR images in 71-year-old man with biopsy-proved HCC in the background of cirrhosis secondary to hemochromatosis. Imaging after RFA of the tumor shows cavity adjacent to the intrahepatic inferior vena cava. RFA cavity (arrow) shows high signal intensity on **(a)** in-phase and **(b)** opposed-phase T1-weighted images (170/4.4–2.2, 70° flip angle) and low signal intensity on **(c)** T2-weighted fast-recovery FSE image (3800/89), indicating coagulative necrosis. Signal intensity loss within the cavity at opposed-phase imaging represents intralesional lipid, which was seen in the tumor prior to ablation. Heterogeneous signal intensity loss in the liver (arrowhead) on in-phase image compared with opposed-phase image is due to iron deposition related to hemochromatosis. Evaluation for enhancement is difficult on **(d)** arterial-dominant phase T1-weighted three-dimensional SPGR image (4.1/1.3, 12° flip angle) due to high-signal-intensity coagulative necrosis within the cavity at precontrast imaging. **(e)** Subtracted image (arterial-phase image minus precontrast image) reveals absent enhancement in the tumor, indicating successful ablation. Compare this lack of enhancement with **(f)** mild tumor enhancement (arrow) on the subtracted image before ablation.

cavity largely reflect coagulative necrosis. The signal intensity of the cavity is predominantly hyperintense compared with surrounding parenchyma on T1-weighted images and hypointense on T2-weighted images (Fig 7). Onishi et al (192) described three zones within the ablation cavity on T1-weighted spoiled gradient-echo images in dogs and one autopsy specimen. These zones include a central zone of low signal intensity, a broad middle hyperintense zone, and a surrounding hypointense band. There was no contrast enhancement of the central and middle zones at administration of gadolinium-based contrast material, and these zones corresponded to coagulative necrosis at pathologic evaluation. The peripheral band corresponded to sinusoidal congestion in the acute phase and to fibrotic changes in the subacute stage, which explains its delayed enhancement with gadolinium-based contrast material. On T2-weighted images, the central and middle zones were of low signal intensity and the peripheral band showed hyperintense signal intensity.

Comparison with preablation images is very important in order to determine the success of ablation. The ablation cavity should correspond to the location of the tumor and be larger in size. Nodular or irregular arterial hypervascularity at the periphery of the cavity with concomitant washout in the venous phase, corresponding to the location and enhancement characteristics of the tumor, indicates residual tumor and incomplete ablation; however, a hyperemic halo can persist around the ablated RFA cavity for several months, which should not be mistaken for tumor recurrence (193). This inflammatory halo persists in the venous and delayed phases of enhancement and is attributed to an inflammatory response and hemorrhagic granulation tissue along the edge of the necrosis. Due to the high signal intensity within the ablation cavity on unenhanced images, assessment of enhancement is often difficult, and subtraction techniques may be helpful (arterial phase gadolinium-enhanced images minus unenhanced images). Careful assessment of the subtracted images for image misregistration is important to avoid overestimation or underestimation of residual enhancement. In our experience, intracellular lipid seen in the original HCC can persist after RFA and appear as signal intensity loss on out-of-phase images compared with in-phase images. Reappearance of irregular enhancement within or at the periphery of the cavity at subsequent follow-up studies usually indicates recurrent tumor.

If the tumor is successfully ablated, the cavity should slightly regress in size with time. Enlargement of the cavity sometimes indicates tumor recurrence (194). Hyperintense signal intensity on T1-weighted images can persist for months or years. The optimal follow-up time is not established. In our practice, we perform imaging follow-up at 6 weeks, at 12 weeks, and then every 3 months.

MR Imaging and Transarterial Chemoembolization

Transarterial chemoembolization is the only therapy associated with increased life expectancy in patients with advanced HCC (195–199). It is recommended by the AASLD as the first-line noncurative therapy for nonsurgical patients with large or multifocal HCC who do not have vascular invasion or extrahepatic spread (20).

HCC exhibits intense neoangiogenic activity during its progression (20). This characteristic provides the rationale to support arterial obstruction as an effective therapeutic option. In this procedure, hepatic artery obstruction by means of transarterial embolization, using usually gelfoam, is combined with prior injection of chemotherapeutic agents, usually doxorubicin, mixed with lipiodol—hence the name transarterial chemoembolization. Selective catheterization of the lobar and segmental branches that feed the tumor is at-

Figure 8

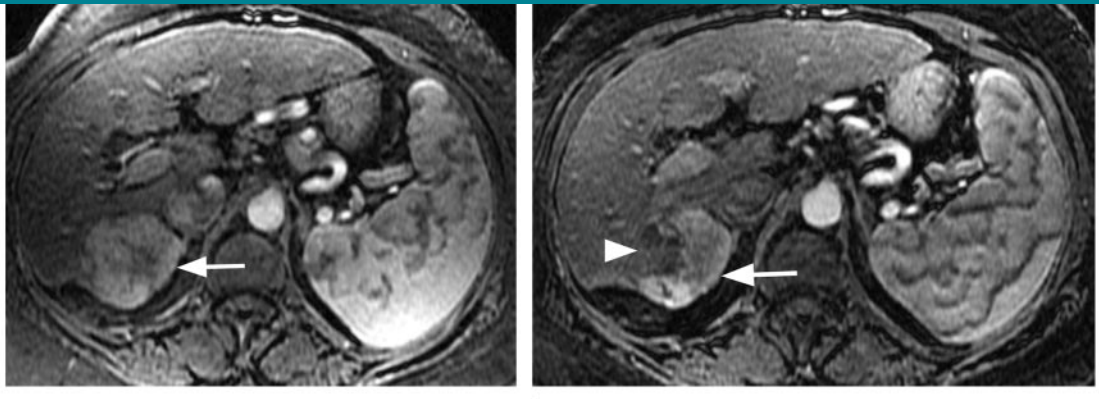

Figure 8: Transverse T1-weighted three-dimensional SPGR MR images in 54-year-old woman with hepatitis C–related cirrhosis and a large HCC in the posterior right lobe treated with chemoembolization. **(a)** Pretreatment image (3.8/1.7, 12° flip angle) acquired in the arterial-dominant phase shows a large hypervascular HCC in the posterior right lobe (arrow). **(b)** Gadolinium-enhanced image (4.2/1.7, 12° flip angle) 12 weeks after chemoembolization shows residual enhancement in 60% of the tumor (arrow) with no enhancement in treated portion of the tumor (arrowhead). This indicates partial response to chemoembolization.

tempted in order to minimize injury to surrounding nontumorous liver. Multifocal HCC may require obstruction of the total hepatic arterial blood flow.

Imaging prior to treatment is performed to assess tumor extent, portal venous thrombosis, and extrahepatic spread. Transarterial chemoembolization induces tumor necrosis in over 50% of patients and an improved survival compared with supportive care (23). Response is indicated by the presence of large necrotic areas within the tumor and reduction in tumor burden on MR or CT images (23) (Fig 8). Lipiodol is best seen on CT images as intense hyperattenuating material at the site of uptake, usually in the region of the tumor, but this can mask enhancement within the cavity. Dynamic contrast-enhanced MR imaging has been shown to be the best modality for the evaluation of arterial enhancement, which indicates residual tumor (200). The presence or absence of residual viable tumor on MR images does not correlate with lipiodol uptake in the same region on CT images (200). Lipiodol produces high signal intensity on T1-weighted images in the first few days after transarterial chemoembolization in areas of uptake within the tumor. This high signal intensity returns to normal at 3 months. Lipiodol does not affect the T2-weighted signal intensity of the tumor (201). We have also noticed loss of signal intensity on out-of-phase images compared with in-phase images in areas of lipiodol uptake. Diffusion-weighted MR imaging and spectroscopy have recently been used to evaluate response to treatment and have shown promising results (202,203).

In summary, over the past few years MR imaging of the liver has progressed substantially. Technical advances in hardware and software have facilitated rapid acquisition of images with excellent anatomic detail. Volumetric sequences enable three-dimensional serial dynamic imaging of the liver to demonstrate the typical vascular features of HCC. Sensitivity remains poor for the detection of small HCC nodules. However, there is increasing recognition of the role of imaging, and of MR imaging in particular, in the surveillance of the cirrhotic liver for nodules, in the diagnosis of HCC, and in the monitoring of lesions following local and systemic treatments.

References

1. Parkin DM, Bray F, Ferlay J, Pisani P. Estimating the world cancer burden: Globocan 2000. Int J Cancer 2001;94(2):153–156.
2. El-Serag HB. Hepatocellular carcinoma: recent trends in the United States. Gastroenterology 2004;127(5 suppl 1):S27–S34.
3. El-Serag HB, Mason AC. Rising incidence of hepatocellular carcinoma in the United States. N Engl J Med 1999;340(10):745–750.
4. Davila JA, Morgan RO, Shaib Y, McGlynn KA, El-Serag HB. Hepatitis C infection and the increasing incidence of hepatocellular carcinoma: a population-based study. Gastroenterology 2004;127(5):1372–1380.
5. Trends in SEER incidence and death rates by primary cancer site 1994–2003: surveillance epidemiology and end results. National Cancer Institute Web site. http://seer.cancer.gov/cgi-bin/csr/1975_2003/search.pl#results. Section 1, page 62. Accessed July 30, 2006.
6. Llovet JM, Burroughs A, Bruix J. Hepatocellular carcinoma. Lancet 2003;362(9399):1907–1917.
7. Deuffic S, Poynard T, Buffat L, Valleron AJ. Trends in primary liver cancer. Lancet 1998;351(9097):214–215.
8. Tanaka Y, Hanada K, Mizokami M, et al. A comparison of the molecular clock of hepatitis C virus in the United States and Japan predicts that hepatocellular carcinoma incidence in the United States will increase over the next two decades. Proc Natl Acad Sci U S A 2002;99(24):15584–15589.
9. Fattovich G, Giustina G, Degos F. Morbidity and mortality in compensated cirrhosis type C: a retrospective follow-up study of 384 patients. Gastroenterology 1997;112(2):463–472.
10. Fattovich G, Stroffolini T, Zagni I, Donato F. Hepatocellular carcinoma in cirrhosis: incidence and risk factors. Gastroenterology 2004;127(5 suppl 1):S35–S50.
11. Beasley RP, Hwang LY, Lin CC, Chien CS. Hepatocellular carcinoma and hepatitis B virus: a prospective study of 22 707 men in Taiwan. Lancet 1981;2(8256):1129–1133.
12. Fattovich G, Giustina G, Schalm SW, et al. Occurrence of hepatocellular carcinoma and decompensation in western European patients with cirrhosis type B. The EUROHEP Study Group on Hepatitis B Virus and Cirrhosis. Hepatology 1995;21(1):77–82.
13. Liaw YF, Tai DI, Chu CM, et al. Early detection of hepatocellular carcinoma in patients with chronic type B hepatitis: a prospective study. Gastroenterology 1986;90(2):263–267.
14. Bosch FX, Ribes J, Díaz M, Clèries R. Primary liver cancer: worldwide incidence and trends. Gastroenterology 2004;127(5 suppl 1):S5–S16.
15. Zhou XD, Tang ZY, Yang BH, et al. Experience of 1000 patients who underwent hepatectomy for small hepatocellular carcinoma. Cancer 2001;91(8):1479–1486.
16. Marrero JA, Fontana RJ, Su GL, Conjeevaram HS, Emick DM, Lok AS. NAFLD may be a common underlying liver disease in patients with hepatocellular carcinoma in the United States. Hepatology 2002;36(6):1349–1354.
17. Meissner HI, Smith RA, Rimer BK, et al. Promoting cancer screening: learning from experience. Cancer 2004;101(5 suppl):1107–1117.
18. Llovet JM, Schwartz M, Mazzaferro V. Resection and liver transplantation for hepatocellular carcinoma. Semin Liver Dis 2005;25(2):181–200.
19. Marrero JA. Screening tests for hepatocellular carcinoma. Clin Liver Dis 2005;9(2):235–251.
20. Bruix J, Sherman M. Practice Guidelines Committee, American Association for the Study of Liver Diseases. Management of hepatocellular carcinoma. Hepatology 2005;42(5):1208–1236.
21. Zhang BH, Yang BH, Tang ZY. Randomized controlled trial of screening for hepatocellular carcinoma. J Cancer Res Clin Oncol 2004;130(7):417–422.
22. Colli A, Fraquelli M, Casazza G, et al. Accuracy of ultrasonography, spiral CT, magnetic resonance, and alpha-fetoprotein in diagnosing hepatocellular carcinoma: a systematic review. Am J Gastroenterol 2006;101(3):513–523.
23. Bruix J, Sherman M, Llovet JM. Clinical management of hepatocellular carcinoma: conclusions of the Barcelona-2000 EASL conference. European Association for the Study of the Liver. J Hepatol 2001;35(3):421–430.
24. Ito K, Mitchell DG. Imaging diagnosis of cirrhosis and chronic hepatitis. Intervirology 2004;47(3-5):134–143.
25. Krinsky GA, Lee VS. MR imaging of cirrhotic nodules. Abdom Imaging 2000;25(5):471–482.
26. Coleman WB. Mechanisms of human hepatocarcinogenesis. Curr Mol Med 2003;3(6):573–588.
27. Efremidis SC, Hytiroglou P. The multistep process of hepatocarcinogenesis in cirrhosis with imaging correlation. Eur Radiol 2002;12(4):753–764.
28. Shah TU, Semelka RC, Pamuklar E, et al. The risk of hepatocellular carcinoma in cirrhotic patients with small liver nodules on MRI. Am J Gastroenterol 2006;101(3):533–540.

29. Terminology of nodular hepatocellular lesions. International Working Party. Hepatology 1995;22(3):983–993.

30. Baron RL, Peterson MS. Screening the cirrhotic liver for hepatocellular carcinoma with CT and MR imaging: opportunities and pitfalls. RadioGraphics 2001;21(Spec Issue):S117–S132.

31. Lim JH, Kim EY, Lee WJ, et al. Regenerative nodules in liver cirrhosis: findings at CT during arterial portography and CT hepatic arteriography with histopathologic correlation. Radiology 1999;210(2):451–458.

32. Freeny PC, Grossholz M, Kaakaji K, Schmiedl UP. Significance of hyperattenuating and contrast-enhancing hepatic nodules detected in the cirrhotic liver during arterial phase helical CT in pre-liver transplant patients: radiologic-histopathologic correlation of explanted livers. Abdom Imaging 2003;28(3):333–346.

33. Krinsky GA, Israel G. Nondysplastic nodules that are hyperintense on T1-weighted gradient-echo MR imaging: frequency in cirrhotic patients undergoing transplantation. AJR Am J Roentgenol 2003;180(4):1023–1027.

34. Mathieu D, Paret M, Mahfouz AE, et al. Hyperintense benign liver lesions on spin-echo T1-weighted MR images: pathologic correlations. Abdom Imaging 1997;22(4):410–417.

35. Zhang J, Krinsky GA. Iron-containing nodules of cirrhosis. NMR Biomed 2004;17(7):459–464.

36. Krinsky GA, Lee VS, Nguyen MT, et al. Siderotic nodules in the cirrhotic liver at MR imaging with explant correlation: no increased frequency of dysplastic nodules and hepatocellular carcinoma. Radiology 2001;218(1):47–53.

37. Ito K, Mitchell DG, Gabata T, et al. Hepatocellular carcinoma: association with increased iron deposition in the cirrhotic liver at MR imaging. Radiology 1999;212(1):235–240.

38. Putative precancerous lesions. In: Ishak KG, Goodman ZD, Stocker JT. Atlas of tumor pathology: tumors of the liver and intrahepatic bile ducts. Third series, fascicle 31. Armed Forces Institute of Pathology, 2001; 185.

39. Theise ND, Schwartz M, Millller C, Thung SN. Macroregenerative nodules and hepatocellular carcinoma in forty-four sequential adult liver explants with cirrhosis. Hepatology 1992;16(4):949–955.

40. Theise ND, Fiel IM, Hytiroglou P, et al. Macroregenerative nodules in cirrhosis are not associated with elevated serum or stainable tissue alpha-fetoprotein. Liver 1995;15(1):30–34.

41. Takayama T, Makuuchi M, Hirohashi S, et al. Malignant transformation of adenomatous hyperplasia to hepatocellular carcinoma. Lancet 1990;336(8724):1150–1153.

42. Sakamoto M, Hirohashi S, Shimosato Y. Early stages of multistep hepatocarcinogenesis: adenomatous hyperplasia and early hepatocellular carcinoma. Hum Pathol 1991;22(2):172–178.

43. Lim JH, Choi BI. Dysplastic nodules in liver cirrhosis: imaging. Abdom Imaging 2002;27(2):117–128.

44. Matsui O, Kadoya M, Kameyama T, et al. Benign and malignant nodules in cirrhotic livers: distinction based on blood supply. Radiology 1991;178(2):493–497.

45. Choi BI, Han JK, Hong SH, et al. Dysplastic nodules of the liver: imaging findings. Abdom Imaging 1999;24(3):250–257.

46. Hayashi M, Matsui O, Ueda K, et al. Correlation between the blood supply and grade of malignancy of hepatocellular nodules associated with liver cirrhosis: evaluation by CT during intraarterial injection of contrast medium. AJR Am J Roentgenol 1999;172(4):969–976.

47. Krinsky GA, Theise ND, Rofsky NM, Mizrachi H, Tepperman LW, Weinreb JC. Dysplastic nodules in cirrhotic liver: arterial phase enhancement at CT and MR imaging—a case report. Radiology 1998;209(2):461–464.

48. Kim T, Baron RL, Nalesnik MA. Infarcted regenerative nodules in cirrhosis: CT and MR imaging findings with pathologic correlation. AJR Am J Roentgenol 2000;175(4):1121–1125.

49. Seki S, Sakaguchi H, Kitada T, et al. Outcomes of dysplastic nodules in human cirrhotic liver: a clinicopathological study. Clin Cancer Res 2000;6(9):3469–3473.

50. Mitchell DG, Rubin R, Siegelman ES, Burk DL Jr, Rifkin MD. Hepatocellular carcinoma within siderotic regenerative nodules: appearance as a nodule within a nodule on MR images. Radiology 1991;178(1):101–103.

51. Goshima S, Kanematsu M, Matsuo M, et al. Nodule-in-nodule appearance of hepatocellular carcinomas: comparison of gadolinium-enhanced and ferumoxides-enhanced magnetic resonance imaging. J Magn Reson Imaging 2004;20(2):250–255.

52. Hepatocellular carcinoma. In: Ishak KG, Goodman ZD, Stocker JT. Atlas of tumor pathology: tumors of the liver and intrahepatic bile ducts. Third series, fascicle 31. Armed Forces Institute of Pathology, 2001; 199–230.

53. Earls JP, Theise ND, Weinreb JC, et al. Dysplastic nodules and hepatocellular carcinoma: thin-section MR imaging of explanted cirrhotic livers with pathologic correlation. Radiology 1996;201(1):207–214.

54. Kelekis NL, Semelka RC, Worawattanakul S, et al. Hepatocellular carcinoma in North America: a multiinstitutional study of appearance on T1-weighted, T2-weighted, and serial gadolinium-enhanced gradient-echo images. AJR Am J Roentgenol 1998;170(4):1005–1013.

55. Kelekis NL, Semelka RC, Woosley JT. Malignant lesions of the liver with high signal intensity on T1-weighted MR images. J Magn Reson Imaging 1996;6(2):291–294.

56. Mitchell DG, Palazzo J, Hann HW, Rifkin MD, Burk DL Jr, Rubin R. Hepatocellular tumors with high signal on T1-weighted MR images: chemical shift MR imaging and histologic correlation. J Comput Assist Tomogr 1991;15(5):762–769.

57. Hussain HK, Syed I, Nghiem HV, et al. T2-weighted MR imaging in the assessment of cirrhotic liver. Radiology 2004;230(3):637–644.

58. Hecht EM, Holland AE, Israel GM, et al. Hepatocellular carcinoma in the cirrhotic liver: gadolinium-enhanced 3D T1-weighted MR imaging as a stand-alone sequence for diagnosis. Radiology 2006;239(2):438–447.

59. Matsui O. Imaging of multistep human hepatocarcinogenesis by CT during intraarterial contrast injection. Intervirology 2004;47(3-5):271–276.

60. Park YN, Yamg CP, Fernandez GJ, Cubukcu O, Thung S, Theise ND. Neoangiogenesis and sinusoidal "capillarization" in dysplastic nodules of the liver. Am J Surg Pathol 1998;22(6):656–662.

61. Shinmura R, Matsui O, Kobayashi S, et al. Cirrhotic nodules: association between MR imaging signal intensity and intranodular blood supply. Radiology 2005;237(2):512–519.

62. Marrero JA, Hussain HK, Nghiem HV, Umar R, Fontana RJ, Lok AS. Improving the prediction of hepatocellular carcinoma in cirrhotic patients with an arterially-enhancing liver mass. Liver Transpl 2005;11(3):281–289.

63. Torimura T, Ueno T, Kin M, et al. Overexpression of angiopoietin-1 and angiopoietin-2 in hepatocellular carcinoma. J Hepatol 2004;40(5):799–807.

64. Organ distribution: allocation of livers—liver transplant candidates with hepatocellular carcinoma (HCC). United Network for Organ Sharing Web site. http://www.unos.org/policiesandbylaws/policies.asp?resources=true. Revised September 18, 2007. Accessed February 27, 2008.

65. Yamashita Y, Mitsuzaki K, Yi T, et al. Small hepatocellular carcinoma in patients with chronic liver damage: prospective comparison of detection with dynamic MR imaging and helical CT of the whole liver. Radiology 1996;200(1):79–84.

66. Peterson MS, Baron RL, Murakami T. Hepatic malignancies: usefulness of acquisition of multiple arterial and portal venous phase images at dynamic gadolinium-enhanced MR imaging. Radiology 1996;201(2):337–345.

67. Murakami T, Kim T, Takamura M, et al. Hypervascular hepatocellular carcinoma: detection with double arterial phase multi–detector row helical CT. Radiology 2001;218(3):763–767.

68. Ito K, Fujita T, Shimizu A, et al. Multiarterial phase dynamic MRI of small early enhancing hepatic lesions in cirrhosis or chronic hepatitis: differentiating between hypervascular hepatocellular carcinomas and pseudolesions. AJR Am J Roentgenol 2004;183(3):699–705.

69. Ito K. Hepatocellular carcinoma: conventional MRI findings including gadolinium-enhanced dynamic imaging. Eur J Radiol 2006;58(2):186–199.

70. Bolondi L, Gaiani S, Celli N, et al. Characterization of small nodules in cirrhosis by assessment of vascularity: the problem of hypovascular hepatocellular carcinoma. Hepatology 2005;42(1):27–34.

71. Holland AE, Hecht EM, Hahn WY, et al. Importance of small (< or = 20-mm) enhancing lesions seen only during the hepatic arterial phase at MR imaging of the cirrhotic liver: evaluation and comparison with whole explanted liver. Radiology 2005; 237(3):938–944.

72. Gryspeerdt S, Van Hoe L, Marchal G, Baert AL. Evaluation of hepatic perfusion disorders with double-phase spiral CT. RadioGraphics 1997;17(2):337–348.

73. Koseoglu K, Taskin F, Ozsunar Y, Cildag B, Karaman C. Transient hepatic attenuation differences at biphasic spiral CT examinations. Diagn Interv Radiol 2005;11(2):96–101.

74. Ito K, Honjo K, Fujita T, Awaya H, Matsumoto T, Matsunaga N. Hepatic parenchymal hyperperfusion abnormalities detected with multisection dynamic MR imaging: appearance and interpretation. J Magn Reson Imaging 1996;6(6): 861–867.

75. Carlos RC, Kim HM, Hussain HK, Francis IR, Nghiem HV, Fendrick AM. Developing a prediction rule to assess hepatic malignancy in patients with cirrhosis. AJR Am J Roentgenol 2003;180(4):893–900.

76. Hwang GJ, Kim MJ, Yoo HS, Lee JT. Nodular hepatocellular carcinomas: detection with arterial-, portal-, and delayed-phase images at spiral CT. Radiology 1997; 202(2):383–388.

77. Lim JH, Choi D, Kim SH, et al. Detection of hepatocellular carcinoma: value of adding delayed phase imaging to dual-phase helical CT. AJR Am J Roentgenol 2002;179(1): 67–73.

78. Iannaccone R, Laghi A, Catalano C, et al. Hepatocellular carcinoma: role of unenhanced and delayed phase multi–detector row helical CT in patients with cirrhosis. Radiology 2005;234(2):460–467.

79. Ueda K, Matsui O, Kawamori Y, et al. Hypervascular hepatocellular carcinoma: evaluation of hemodynamics with dynamic CT during hepatic arteriography. Radiology 1998;206(1):161–166.

80. Stevens WR, Gulino SP, Batts KP, Stephens DH, Johnson CD. Mosaic pattern of hepatocellular carcinoma: histologic basis for a characteristic CT appearance. J Comput Assist Tomogr 1996;20(3):337–342.

81. Kanematsu M, Semelka RC, Leonardou P, Mastropasqua M, Lee JK. Hepatocellular carcinoma of diffuse type: MR imaging findings and clinical manifestations. J Magn Reson Imaging 2003;18(2):189–195.

82. Dodd GD 3rd, Memel DS, Baron RL, Eichner L, Santiguida LA. Portal vein thrombosis in patients with cirrhosis: does sonographic detection of intrathrombus flow allow differentiation of benign and malignant thrombus? AJR Am J Roentgenol 1995;165(3):573–577.

83. Amitrano L, Guardascione MA, Brancaccio V, et al. Risk factors and clinical presentation of portal vein thrombosis in patients with cirrhosis. J Hepatol 2004;40(5):736–741.

84. Manzanet G, Sanjuan F, Orbis P, et al. Liver transplantation in patients with portal vein thrombosis. Liver Transpl 2001;7(2): 125–131.

85. Takayasu K, Arii S, Ikai I, et al. Prospective cohort study of transarterial chemoembolization for unresectable hepatocellular carcinoma in 8510 patients. Gastroenterology 2006;131(2):461–469.

86. Koike Y, Nakagawa K, Shiratori Y, et al. Factors affecting the prognosis of patients with hepatocellular carcinoma invading the portal vein: a retrospective analysis using 952 consecutive HCC patients. Hepatogastroenterology 2003;50(54):2035–2039.

87. Pirisi M, Avellini C, Fabris C, et al. Portal vein thrombosis in hepatocellular carcinoma: age and sex distribution in an autopsy study. J Cancer Res Clin Oncol 1998;124(7):397–400.

88. Llovet JM, Bustamante J, Castells A, et al. Natural history of untreated nonsurgical hepatocellular carcinoma: rationale for the design and evaluation of therapeutic trials. Hepatology 1999;29(1):62–67.

89. Nakashima T, Okuda K, Kojiro M, et al. Pathology of hepatocellular carcinoma in Japan: 232 consecutive cases autopsied in ten years. Cancer 1983;51(5):863–877.

90. Tublin ME, Dodd GD 3rd, Baron RL. Benign and malignant portal vein thrombosis: differentiation by CT characteristics. AJR Am J Roentgenol 1997;168(3):719–723.

91. Aslam Sohaib SA, Teh J, Nargund VH, Lumley JS, Hendry WF, Reznek RH. Assessment of tumor invasion of the vena caval wall in renal cell carcinoma cases by magnetic resonance imaging. J Urol 2002; 167(3):1271–1275.

92. Park JH, Koh KC, Choi MS, et al. Analysis of risk factors associated with early multinodular recurrences after hepatic resection for hepatocellular carcinoma. Am J Surg 2006;192(1):29–33.

93. Kim BW, Kim YB, Wang HJ, Kim MW. Risk factors for immediate post-operative fatal recurrence after curative resection of hepatocellular carcinoma. World J Gastroenterol 2006;12(1):99–104.

94. Vauthey JN, Klimstra D, Franceschi D, et al. Factors affecting long-term outcome after hepatic resection for hepatocellular carcinoma. Am J Surg 1995;169(1):28–34.

95. Okada S, Shimada K, Yamamoto J, et al. Predictive factors for postoperative recurrence of hepatocellular carcinoma. Gastroenterology 1994;106(6):1618–1624.

96. Itai Y, Matsui O. Blood flow and liver imaging. Radiology 1997;202(2):306–314.

97. Schlund JF, Semelka RC, Kettritz U, Eisenberg LB, Lee JK. Transient increased segmental hepatic enhancement distal to portal vein obstruction on dynamic gadolinium-enhanced gradient-echo MR images. J Magn Reson Imaging 1995;5(4):375–377.

98. Wiesner RH, Freeman RB, Mulligan DC. Liver transplantation for hepatocellular cancer: the impact of the MELD allocation policy. Gastroenterology 2004;127(5 suppl 1):S261–S267.

99. Krinsky GA, Lee VS, Theise ND, et al. Hepatocellular carcinoma and dysplastic nodules in patients with cirrhosis: prospective diagnosis with MR imaging and explantation correlation. Radiology 2001;219(2): 445–454.

100. Brancatelli G, Baron RL, Peterson MS, Marsh W. Helical CT screening for hepatocellular carcinoma in patients with cirrhosis: frequency and causes of false-positive interpretation. AJR Am J Roentgenol 2003;180(4):1007–1014.

101. Yu JS, Kim KW, Jeong MG, Lee JT, Yoo HS. Nontumorous hepatic arterial-portal venous shunts: MR imaging findings. Radiology 2000;217(3):750–756.

102. Yu JS, Kim KW, Sung KB, Lee JT, Hyung SY. Small arterial-porta venous shunts: a cause of pseudolesions at hepatic imaging. Radiology 1997;203(3):737–742.

103. Baron RL. Understanding and optimizing use of contrast material for CT of the liver. AJR Am J Roentgenol 1994;163(2):323–331.

104. Dodd GD 3rd, Baron RL, Oliver JH 3rd, Federle MP. Spectrum of imaging findings of the liver in end-stage cirrhosis. I. Gross morphology and diffuse abnormalities. AJR Am J Roentgenol 1999;173(4):1031–1036.

105. Ahn IO, de Lange EE. Early hyperenhancement of confluent hepatic fibrosis on dynamic MR imaging. AJR Am J Roentgenol 1998;171(3):901–902.

106. Brancatelli G, Federle MP, Baron RL, Lagalla R, Midiri M, Vilgrain V. Arterially enhancing liver lesions: significance of sustained enhancement on hepatic venous and delayed phase with magnetic resonance imaging. J Comput Assist Tomogr 2007;31(1): 116–124.

107. Dodd GD 3rd, Baron RL, Oliver JH 3rd, Federle MP. Spectrum of imaging findings of the liver in end-stage cirrhosis. II. Focal

abnormalities. AJR Am J Roentgenol 1999; 173(5):1185–1192.

108. Quaglia A, Tibballs J, Grasso A, et al. Focal nodular hyperplasia-like areas in cirrhosis. Histopathology 2003;42(1):14–21.

109. Seymour K, Charnley RM. Evidence that metastasis is less common in cirrhotic than normal liver: a systematic review of post-mortem case-control studies. Br J Surg 1999;86(10):1237–1242.

110. Ruiz Guinaldo A, Martin Herrera L, Roldan Cuadra R. Hepatic tumors in patients with cirrhosis: an autopsy study. Rev Esp Enferm Dig 1997;89(10):771–780.

111. Vilgrain V, Lewin M, Vons C, et al. Hepatic nodules in Budd-Chiari syndrome: imaging features. Radiology 1999;210(2):443–450.

112. Reshamwala PA, Kleiner DE, Heller T. Nodular regenerative hyperplasia: not all nodules are created equal. Hepatology 2006;44(1):7–14.

113. Maetani Y, Itoh K, Egawa H, et al. Benign hepatic nodules in Budd-Chiari syndrome: radiologic-pathologic correlation with emphasis on the central scar. AJR Am J Roentgenol 2002;178(4):869–875.

114. Choi BI, Lee JM, Han JK. Imaging of intrahepatic and hilar cholangiocarcinoma. Abdom Imaging 2004;29(5):548–557.

115. Blachar A, Federle MP, Brancatelli G. Hepatic capsular retraction: spectrum of benign and malignant etiologies. Abdom Imaging 2002;27(6):690–699.

116. Hussain SM, Wielopolski PA, Martin DR. Abdominal magnetic resonance imaging at 3.0T: problem or a promise for the future? Top Magn Reson Imaging 2005;16(4):325–335.

117. Martin DR, Danrad R, Hussain SM. MR imaging of the liver. Radiol Clin North Am 2005;43(5):861–886.

118. Kimura T, Hirokawa Y, Murakami Y, et al. Reproducibility of organ position using voluntary breath-hold method with spirometer for extracranial stereotactic radiotherapy. Int J Radiat Oncol Biol Phys 2004;60(4): 1307–1313.

119. Rofsky NM, Weinreb JC, Ambrosino MM, Safir J, Krinsky G. Comparison between in-phase and opposed-phase T1-weighted breath-hold FLASH sequences for hepatic imaging. J Comput Assist Tomogr 1996; 20(2):230–235.

120. Merkle EM, Nelson RC. Dual gradient-echo in-phase and opposed-phase hepatic MR imaging: a useful tool for evaluating more than fatty infiltration and fatty sparing. RadioGraphics 2006;26(5):1409–1418.

121. Rofsky NM, Lee VS, Laub G, et al. Abdominal MR imaging with volumetric interpolated breath-hold examination. Radiology 1999;212(3):876–884.

122. Lee VS, Lavelle MT, Rofsky NM, et al. Hepatic MR imaging with a dynamic contrast-enhanced isotropic volumetric interpolated breath-hold examination: feasibility, reproducibility, and technical quality. Radiology 2000;215(2):365–372.

123. Blasbalg R, Mitchell DG, Outwater EK, Ito K, Gabata T, Chiowanich P. Free MRA of the abdomen: post processing dynamic gadolinium-enhanced 3D axial MR images. Abdom Imaging 2000;25(1):62–66.

124. Lavelle MT, Lee VS, Rofsky NM, Keinsky GA, Weinreb JC. Dynamic contrast-enhanced three dimensional MR imaging of liver parenchyma: source images and angiographic reconstructions to define hepatic arterial anatomy. Radiology 2001; 218(2):389–394.

125. Earls JP, Rofsky NM, DeCorato DR, Krinsky GA, Weinreb JC. Hepatic arterial-phase dynamic gadolinium-enhanced MR imaging: optimization with a test examination and power injector. Radiology 1997;202(1): 268–273.

126. Hussain HK, Londy FJ, Francis IR, et al. Hepatic arterial phase MR imaging with automated bolus detection and three-dimensional fast gradient-recalled-echo sequences: comparison with test-bolus method. Radiology 2003; 226(2):558–566.

127. Mori K, Yoshioka H, Takahashi N, et al. Triple arterial phase dynamic MRI with sensitivity encoding for hypervascular hepatocellular carcinoma: comparison of the diagnostic accuracy among the early, middle, late, and whole triple arterial phase imaging. AJR Am J Roentgenol 2005;184(1):63–69.

128. Vogt FM, Antoch G, Hunold P, et al. Parallel acquisition techniques for accelerated volumetric interpolated breath-hold examination magnetic resonance imaging of the upper abdomen: assessment of image quality and lesion conspicuity. J Magn Reson Imaging 2005;21(4):376–382.

129. Yu JS, Kim YH, Rofsky NM. Dynamic subtraction magnetic resonance imaging of cirrhotic liver: assessment of high signal intensity lesions on nonenhanced T1-weighted images. J Comput Assist Tomogr 2005; 29(1):51–58.

130. Krinsky GA, Lee VS, Theise ND, et al. Transplantation for hepatocellular carcinoma and cirrhosis: sensitivity of magnetic resonance imaging. Liver Transpl 2002; 8(12):1156–1164.

131. Burrel M, Llovet JM, Ayuso C, et al. MRI angiography is superior to helical CT for detection of HCC prior to liver transplantation: an explant correlation. Hepatology 2003;38(4): 1034–1042.

132. de Ledinghen V, Laharie D, Lecesne R, et al. Detection of nodules in liver cirrhosis: spiral computed tomography or magnetic resonance imaging? a prospective study of 88 nodules in 34 patients. Eur J Gastroenterol Hepatol 2002;14(2):159–165.

133. Tomemori T, Yamakado K, Nakatsuka A, Sakuma H, Matsumura K, Takeda K. Fast 3D dynamic MR imaging of the liver with MR SmartPrep: comparison with helical CT in detecting hypervascular hepatocellular carcinoma. Clin Imaging 2001;25(5):355–361.

134. Rode A, Bancel B, Douek P, et al. Small nodule detection in cirrhotic livers: evaluation with US, spiral CT, and MRI and correlation with pathologic examination of explanted liver. J Comput Assist Tomogr 2001;25(3):327–336.

135. Noguchi Y, Murakami T, Kim T, et al. Detection of hepatocellular carcinoma: comparison of dynamic MR imaging with dynamic double arterial phase helical CT. AJR Am J Roentgenol 2003;180(2):455–460.

136. Noguchi Y, Murakami T, Kim T, et al. Detection of hypervascular hepatocellular carcinoma by dynamic magnetic resonance imaging with double-echo chemical shift in-phase and opposed-phase gradient echo technique: comparison with dynamic helical computed tomography imaging with double arterial phase. J Comput Assist Tomogr 2002;26(6):981–987.

137. Libbrecht L, Bielen D, Verslype C, et al. Focal lesions in cirrhotic explant livers: pathological evaluation and accuracy of pretransplantation imaging examinations. Liver Transpl 2002;8(9):749–761.

138. Teefey SA, Hildeboldt CC, Dehdashti F, et al. Detection of primary hepatic malignancy in liver transplant candidates: prospective comparison of CT, MR imaging, US, and PET. Radiology 2003;226(2):533–542.

139. Kim YK, Kwak HS, Kim CS, Chung GH, Han YM, Lee JM. Hepatocellular carcinoma in patients with chronic liver disease: comparison of SPIO-enhanced MR imaging and 16–detector row CT. Radiology 2006; 238(2):531–541.

140. Ward J, Guthrie JA, Scott DJ, et al. Hepatocellular carcinoma in the cirrhotic liver: double-contrast MR imaging for diagnosis. Radiology 2000;216(1):154–162.

141. Bhartia B, Ward J, Guthrie JA, Robinson PJ. Hepatocellular carcinoma in cirrhotic livers double-contrast thin-section MR imaging with pathologic correlation of explanted tissue. AJR Am J Roentgenol 2003; 180(3):577–584.

142. Marrero JA, Fontana RJ, Barrat A, et al. Prognosis of hepatocellular carcinoma: comparison of 7 staging systems in an American cohort. Hepatology 2005;41(4): 707–716.

143. Mazzaferro V, Regalia E, Doci R, et al. Liver transplantation for the treatment of small hepatocellular carcinomas in patients with cirrhosis. N Engl J Med 1996;334(11): 693–699.

144. Marrero JA. Hepatocellular carcinoma. Curr Opin Gastroenterol 2006;22(3):248–253.

145. Cillo U, Vitale A, Grigoletto F, et al. Prospective validation of the Barcelona Clinic Liver Cancer staging system. J Hepatol 2006;44(4):723–731.

146. Grieco A, Pompili M, Caminiti G, et al. Prognostic factors for survival in patients with early-intermediate hepatocellular carcinoma undergoing non-surgical therapy: comparison of Okuda, CLIP, and BCLC staging systems in a single Italian centre. Gut 2005;54(3):411–418.

147. Sala M, Forner A, Varela M, Bruix J. Prognostic prediction in patients with hepatocellular carcinoma. Semin Liver Dis 2005; 25(2):171–180.

148. Kamath PS, Wiesner RH, Malinchoc M, et al. A model to predict survival in patients with end-stage liver disease. Hepatology 2001;33(2):464–470.

149. Wiesner RH. Patient selection in an era of donor liver shortage: current US policy. Nat Clin Pract Gastroenterol Hepatol 2005; 2(1):24–30.

150. Shimizu A, Ito K, Koike S, Fujita T, Shimizu K, Matsunaga N. Cirrhosis or chronic hepatitis: evaluation of small (≤2-cm) early-enhancing hepatic lesions with serial contrast-enhanced dynamic MR imaging. Radiology 2003;226(2): 550–555.

151. Jeong YY, Mitchell DG, Kamishima T. Small (<20 mm) enhancing hepatic nodules seen on arterial phase MR imaging of the cirrhotic liver: clinical implications. AJR Am J Roentgenol 2002;178(6):1327–1334.

152. Taouli B, Losada M, Holland A, Krinsky G. Magnetic resonance imaging of hepatocellular carcinoma. Gastroenterology 2004; 127(5 suppl 1):S144–S152.

153. Taouli B, Goh JS, Lu Y, et al. Growth rate of hepatocellular carcinoma: evaluation with serial computed tomography or magnetic resonance imaging. J Comput Assist Tomogr 2005;29(4):425–429.

154. Arii S, Yamaoka Y, Futagawa S, et al. Results of surgical and nonsurgical treatment for small-sized hepatocellular carcinomas: a retrospective and nationwide survey in Japan. The Liver Cancer Study Group of Japan. Hepatology 2000;32(6):1224–1229.

155. Ikai I, Arii S, Kojiro M, et al. Reevaluation of prognostic factors for survival after liver resection in patients with hepatocellular carcinoma in a Japanese nationwide survey. Cancer 2004;101(4):796–802.

156. Chang S, Kim SH, Lim HK, Lee WJ, Choi D, Lim JH. Needle tract implantation after sonographically guided percutaneous biopsy of hepatocellular carcinoma: evaluation of doubling time, frequency, and features on CT. AJR Am J Roentgenol 2005; 185(2):400–405.

157. O'Malley ME, Takayama Y, Sherman M. Outcome of small (10–20 mm) arterial phase-enhancing nodules seen on triphasic liver CT in patients with cirrhosis or chronic liver disease. Am J Gastroenterol 2005;100(7):1523–1528.

158. Sheu JC, Sung JL, Chen DS, et al. Growth rate of asymptomatic hepatocellular carcinoma and its clinical implications. Gastroenterology 1985;89(2):259–266.

159. Ebara M, Ohto M, Shinagawa T, et al. Natural history of minute hepatocellular carcinoma smaller than three centimeters complicating cirrhosis: a study in 22 patients. Gastroenterology 1986;90(2):289–298.

160. Okazaki N, Yoshino M, Yoshida T, et al. Evaluation of the prognosis for small hepatocellular carcinoma based on tumor volume doubling time: a preliminary report. Cancer 1989;63(11):2207–2210.

161. Barbara L, Benzi G, Gaiani S, et al. Natural history of small untreated hepatocellular carcinoma in cirrhosis: a multivariate analysis of prognostic factors of tumor growth rate and patient survival. Hepatology 1992; 16(1):132–137.

162. Kubota K, Ina H, Okada Y, Irie T. Growth rate of primary single hepatocellular carcinoma: determining optimal screening interval with contrast enhanced computed tomography. Dig Dis Sci 2003;48(3):581–586.

163. Mueller GC, Hussain HK, Carlos RC, Nghiem HV, Francis IR. Effectiveness of MR imaging in characterizing small hepatic lesions: routine versus expert interpretation. AJR Am J Roentgenol 2003;180(3): 673–680.

164. Torzilli G, Minagawa M, Takayama T, et al. Accurate preoperative evaluation of liver mass lesions without fine-needle biopsy. Hepatology 1999;30(4):889–893.

165. Stigliano R, Burroughs AK. Should we biopsy each liver mass suspicious for HCC before liver transplantation?: no, please don't. J Hepatol 2005;43(4):563–568.

166. Marsh JW, Dvorchik I. Should we biopsy each liver mass suspicious for hepatocellular carcinoma before liver transplantation?: yes. J Hepatol 2005;43(4):558–562.

167. Marrero JA, Lok AS. Newer markers for hepatocellular carcinoma. Gastroenterology 2004;127(5 suppl 1):S113–S119.

168. Llovet JM, Fuster J, Bruix J. Intention-to-treat analysis of surgical treatment for early hepatocellular carcinoma: resection versus transplantation. Hepatology 1999; 30(6):1434–1440.

169. Shirabe K, Kanematsu T, Matsumata T, Adachi E, Akazawa K, Sugimachi K. Factors linked to early recurrence of small hepatocellular carcinoma after hepatectomy: univariate and multivariate analyses. Hepatology 1991;14(5):802–805.

170. Poon RT, Fan ST, Lo CM, Liu CL, Wong J. Intrahepatic recurrence after curative resection of hepatocellular carcinoma: long-term results of treatment and prognostic factors. Ann Surg 1999;229(2):216–222.

171. Imamura H, Matsuyama Y, Tanaka E, et al. Risk factors contributing to early and late phase intrahepatic recurrence of hepatocellular carcinoma after hepatectomy. J Hepatol 2003;38(2):200–207.

172. Poon RT, Fan ST, Lo CM, Liu CL, Wong J. Long-term survival and pattern of recurrence after resection of small hepatocellular carcinoma in patients with preserved liver function: implications for a strategy of salvage transplantation. Ann Surg 2002; 235(3):373–382.

173. Livraghi T, Giorgio A, Marin G, et al. Hepatocellular carcinoma and cirrhosis in 746 patients: long-term results of percutaneous ethanol injection. Radiology 1995;197(1): 101–108.

174. Fisher RA, Maluf D, Cotterell AH, et al. Non-resective ablation therapy for hepatocellular carcinoma: effectiveness measured by intention-to-treat and dropout from liver transplant waiting list. Clin Transplant 2004;18(5):502–512.

175. Brillet PY, Paradis V, Brancatelli G, et al. Percutaneous radiofrequency ablation for hepatocellular carcinoma before liver transplantation: a prospective study with histopathologic comparison. AJR Am J Roentgenol 2006;186(5 suppl):S296–S305.

176. Huang GT, Lee PH, Tsang YM, et al. Percutaneous ethanol injection versus surgical resection for the treatment of small hepatocellular carcinoma: a prospective study. Ann Surg 2005;242(1):36–42.

177. Livraghi T, Goldberg SN, Lazzaroni S, Meloni F, Solbiati L, Gazelle GS. Small hepatocellular carcinoma: treatment with radio-frequency ablation versus ethanol injection. Radiology 1999;210(3):655–661.

178. Clark HP, Carson WF, Kavanagh PV, Ho CP, Shen P, Zagoria RJ. Staging and current treatment of hepatocellular carcinoma. RadioGraphics 2005;25(Spec Issue): S3–S23.

179. Dodd GD 3rd, Soulen MC, Kane RA, et al. Minimally invasive treatment of malignant hepatic tumors: at the threshold of a major breakthrough. RadioGraphics 2000;20(1): 9–27.

180. Lu DS, Yu NC, Raman SS, et al. Radiofrequency ablation of hepatocellular carcinoma: treatment success as defined by histologic examination of the explanted liver. Radiology 2005;234(3):954–960.

181. Buscarini L, Buscarini E, Di Stasi M, Vallisa D, Quaretti P, Rocca A. Percutaneous radiofrequency ablation of small hepatocellular carcinoma: long-term results. Eur Radiol 2001;11(6):914–921.

182. Livraghi T, Goldberg SN, Lazzaroni S, et al. Hepatocellular carcinoma: radio-frequency ablation of medium and large lesions. Radiology 2000;214(3):761–768.

183. Mazzaferro V, Battiston C, Perrone S, et al. Radiofrequency ablation of small hepatocellular carcinoma in cirrhotic patients awaiting transplantation: a prospective study. Ann Surg 2004;240(5):900–909.

184. Fontana RJ, Hamidullah H, Nghiem H, et al. Percutaneous radiofrequency thermal ablation of hepatocellular carcinoma: a safe and effective bridge to transplantation. Liver Transpl 2002;8(12):1165–1174.

185. Llovet JM, Schwartz M, Fuster J, Bruix J. Expanded criteria for hepatocellular carcinoma through down-staging prior to liver transplantation: not yet there. Semin Liver Dis 2006;26(3):248–253.

186. Livraghi T, Solbiati L, Meloni MF, Gazelle GS, Halpern EF, Goldberg SN. Treatment of focal liver tumors with percutaneous radio-frequency ablation: complications encountered in a multicenter study. Radiology 2003;226(2):441–451.

187. Giorgio A, Tarantino L, de Stefano G, Coppola C, Ferraioli G. Complications after percutaneous saline-enhanced radiofrequency ablation of liver tumors: 3-year experience with 336 patients at a single center. AJR Am J Roentgenol 2005; 184(1):207–211.

188. Tateishi R, Shiina S, Teratani T, et al. Percutaneous radiofrequency ablation for hepatocellular carcinoma: an analysis of 1000 cases. Cancer 2005;103(6):1201–1209.

189. Llovet JM, Vilana R, Bru C, et al. Increased risk of tumor seeding after percutaneous radiofrequency ablation for single hepatocellular carcinoma. Hepatology 2001;33(5): 1124–1129.

190. Yamasaki T, Kurokawa F, Shirahashi H, Kusano N, Hironaka K, Okita K. Percutaneous radiofrequency ablation therapy for patients with hepatocellular carcinoma during occlusion of hepatic blood flow: comparison with standard percutaneous radiofrequency ablation therapy. Cancer 2002; 95(11):2353–2360.

191. Dromain C, de Baere T, Elias D, et al. Hepatic tumors treated with percutaneous radio-frequency ablation: CT and MR imaging follow-up. Radiology 2002;223(1):255–262.

192. Onishi H, Matsushita M, Murakami T, et al. MR appearances of radiofrequency thermal ablation region: histopathologic correlation with dog liver models and an autopsy case. Acad Radiol 2004;11(10):1180–1189.

193. Goldberg SN, Gazelle GS, Compton CC, Mueller PR, Tanabe KK. Treatment of intrahepatic malignancy with radiofrequency ablation: radiologic-pathologic correlation. Cancer 2000;88(11):2452–2463.

194. Nghiem HV, Francis IR, Fontana R, et al. Computed tomography appearances of hypervascular hepatic tumors after percutaneous radiofrequency ablation therapy. Curr Probl Diagn Radiol 2002;31(3):105–111.

195. Lo CM, Ngan H, Tso WK, et al. Randomized controlled trial of transarterial lipiodol chemoembolization for unresectable hepatocellular carcinoma. Hepatology 2002; 35(5):1164–1171.

196. Bruix J, Sala M, Llovet JM. Chemoembolization for hepatocellular carcinoma. Gastroenterology 2004;127(5 suppl 1):S179–S188.

197. Llovet JM, Bruix J. Systematic review of randomized trials for unresectable hepatocellular carcinoma: chemoembolization improves survival. Hepatology 2003;37(2): 429–442.

198. Llovet JM, Real MI, Montana X, et al. Arterial embolisation or chemoembolisation versus symptomatic treatment in patients with unresectable hepatocellular carcinoma: a randomised controlled trial. Lancet 2002;359(9319): 1734–1739.

199. Lubienski A. Hepatocellular carcinoma: interventional bridging to liver transplantation. Transplantation 2005;80(1 suppl): S113–S119.

200. Kubota K, Hisa N, Nishikawa T, et al. Evaluation of hepatocellular carcinoma after treatment with transcatheter arterial chemoembolization: comparison of lipiodol CT, power Doppler sonography, and dynamic MRI. Abdom Imaging 2001;26(2): 184–190.

201. De Santis M, Alborino S, Tartoni PL, Torricelli P, Casolo A, Romagnoli R. Effects of lipiodol retention on MRI signal intensity from hepatocellular carcinoma and surrounding liver treated by chemoembolization. Eur Radiol 1997;7(1):10–16.

202. Kamel IR, Bluemke DA, Eng J, et al. The role of functional MR imaging in the assessment of tumor response after chemoembolization in patients with hepatocellular carcinoma. J Vasc Interv Radiol 2006;17(3): 505–512.

203. Chen CY, Li CW, Kuo YT, et al. Early response of hepatocellular carcinoma to transcatheter arterial chemoembolization: choline levels and MR diffusion constants–initial experience. Radiology 2006;239(2): 448–456.

Radiology 2008

This is your reprint order form or pro forma invoice

(Please keep a copy of this document for your records.)

Reprint order forms and purchase orders or prepayments must be received 72 hours after receipt of form either by mail or by fax at 410-820-9765. It is the policy of Cadmus Reprints to issue one invoice per order. **Please print clearly**.

Author Name _____
Title of Article _____
Issue of Journal_____ Reprint # _____ Publication Date _____
Number of Pages_____ KB # _____ Symbol Radiology
Color in Article? Yes / No (Please Circle)

Please include the journal name and reprint number or manuscript number on your purchase order or other correspondence.

Order and Shipping Information

Reprint Costs (Please see page 2 of 2 for reprint costs/fees.)

_____ Number of reprints ordered $_____
_____ Number of color reprints ordered $_____
_____ Number of covers ordered $_____
Subtotal $_____
Taxes $_____

(*Add appropriate sales tax for Virginia, Maryland, Pennsylvania, and the District of Columbia or Canadian GST to the reprints if your order is to be shipped to these locations*.)

First address included, add $32 for each additional shipping address $_____

TOTAL $_____

Shipping Address (cannot ship to a P.O. Box) Please Print Clearly

Name _____
Institution _____
Street _____
City _____ State _____ Zip _____
Country _____
Quantity_____ Fax _____
Phone: Day _____ Evening _____
E-mail Address _____

Additional Shipping Address* (cannot ship to a P.O. Box)

Name _____
Institution _____
Street _____
City _____ State _____ Zip _____
Country _____
Quantity _____ Fax _____
Phone: Day _____ Evening _____
E-mail Address _____
** Add $32 for each additional shipping address*

Payment and Credit Card Details

Enclosed: Personal Check _____
Credit Card Payment Details _____
Checks must be paid in U.S. dollars and drawn on a U.S. Bank.

Credit Card: __ VISA __ Am. Exp. __ MasterCard
Card Number _____
Expiration Date_____
Signature: _____

Please send your order form and prepayment made payable to:

Cadmus Reprints
P.O. Box 751903
Charlotte, NC 28275-1903

Note: Do not send express packages to this location, PO Box.
FEIN #:541274108

Invoice or Credit Card Information

Invoice Address Please Print Clearly
Please complete Invoice address as it appears on credit card statement

Name _____
Institution _____
Department _____
Street _____
City _____ State _____ Zip _____
Country _____
Phone _____ Fax _____
E-mail Address _____

Cadmus will process credit cards and *Cadmus Journal Services* will appear on the credit card statement.

If you don't mail your order form, you may fax it to 410-820-9765 with your credit card information.

Signature _____ Date _____

Signature is required. By signing this form, the author agrees to accept the responsibility for the payment of reprints and/or all charges described in this document.

RB-9/26/07

Radiology 2008

Black and White Reprint Prices

Domestic (USA only)						
# of Pages	50	100	200	300	400	500
1-4	$221	$233	$268	$285	$303	$323
5-8	$355	$382	$432	$466	$510	$544
9-12	$466	$513	$595	$652	$714	$775
13-16	$576	$640	$749	$830	$912	$995
17-20	$694	$775	$906	$1,017	$1,117	$1,220
21-24	$809	$906	$1,071	$1,200	$1,321	$1,471
25-28	$928	$1,041	$1,242	$1,390	$1,544	$1,688
29-32	$1,042	$1,178	$1,403	$1,568	$1,751	$1,924
Covers	$97	$118	$215	$323	$442	$555

International (includes Canada and Mexico)						
# of Pages	50	100	200	300	400	500
1-4	$272	$283	$340	$397	$446	$506
5-8	$428	$455	$576	$675	$784	$884
9-12	$580	$626	$805	$964	$1,115	$1,278
13-16	$724	$786	$1,023	$1,232	$1,445	$1,652
17-20	$878	$958	$1,246	$1,520	$1,774	$2,030
21-24	$1,022	$1,119	$1,474	$1,795	$2,108	$2,426
25-28	$1,176	$1,291	$1,700	$2,070	$2,450	$2,813
29-32	$1,316	$1,452	$1,936	$2,355	$2,784	$3,209
Covers	$156	$176	$335	$525	$716	$905

Minimum order is 50 copies. For orders larger than 500 copies, please consult Cadmus Reprints at 800-407-9190.

Reprint Cover

Cover prices are listed above. The cover will include the publication title, article title, and author name in black.

Shipping

Shipping costs are included in the reprint prices. Domestic orders are shipped via UPS Ground service. Foreign orders are shipped via a proof of delivery air service.

Multiple Shipments

Orders can be shipped to more than one location. Please be aware that it will cost $32 for each additional location.

Delivery

Your order will be shipped within 2 weeks of the journal print date. Allow extra time for delivery.

Color Reprint Prices

Domestic (USA only)						
# of Pages	50	100	200	300	400	500
1-4	$223	$239	$352	$473	$597	$719
5-8	$349	$401	$601	$849	$1,099	$1,349
9-12	$486	$517	$852	$1,232	$1,609	$1,992
13-16	$615	$651	$1,105	$1,609	$2,117	$2,624
17-20	$759	$787	$1,357	$1,997	$2,626	$3,260
21-24	$897	$924	$1,611	$2,376	$3,135	$3,905
25-28	$1,033	$1,071	$1,873	$2,757	$3,650	$4,536
29-32	$1,175	$1,208	$2,122	$3,138	$4,162	$5,180
Covers	$97	$118	$215	$323	$442	$555

International (includes Canada and Mexico))						
# of Pages	50	100	200	300	400	500
1-4	$278	$290	$424	$586	$741	$904
5-8	$429	$472	$746	$1,058	$1,374	$1,690
9-12	$604	$629	$1,061	$1,545	$2,011	$2,494
13-16	$766	$797	$1,378	$2,013	$2,647	$3,280
17-20	$945	$972	$1,698	$2,499	$3,282	$4,069
21-24	$1,110	$1,139	$2,015	$2,970	$3,921	$4,873
25-28	$1,290	$1,321	$2,333	$3,437	$4,556	$5,661
29-32	$1,455	$1,482	$2,652	$3,924	$5,193	$6,462
Covers	$156	$176	$335	$525	$716	$905

Tax Due

Residents of Virginia, Maryland, Pennsylvania, and the District of Columbia are required to add the appropriate sales tax to each reprint order. For orders shipped to Canada, please add 7% Canadian GST unless exemption is claimed.

Ordering

Reprint order forms and purchase order or prepayment is required to process your order. Please reference journal name and reprint number or manuscript number on any correspondence. You may use the reverse side of this form as a proforma invoice. Please return your order form and prepayment to:

Cadmus Reprints
P.O. Box 751903
Charlotte, NC 28275-1903

Note: Do not send express packages to this location, PO Box.
FEIN #:541274108

Please direct all inquiries to:

Rose A. Baynard
800-407-9190 (toll free number)
410-819-3966 (direct number)
410-820-9765 (FAX number)
baynardr@cadmus.com (e-mail)

Reprint Order Forms and purchase order or prepayments must be received 72 hours after receipt of form.